

FOR REFERENCE

NOT TO BE TAKEN FROM THIS ROOM

ATMOSPHERIC EFFECTS ON PROPAGATION
DUE TO DIFFERENT PARTICLE SHAPES

by

Osman YILDIRIM

B.S. in E.E. , Boğaziçi University, 1983

Submitted to the Institute for Graduate
Studies in Science and Engineering in
partial fulfillment of the requirements
for degree of

Bogazici University Library



39001100313397

14

Master of Science

in

Electrical Engineering

Boğaziçi University

1986

ACKNOWLEDGEMENTS

I would like to express my sincere gratitude to those who have helped me during the development of this study, especially to my thesis supervisor Assoc Prof. Selim ŞEKER for his kind interest and invaluable aid.

I am also indebted to Turkish Air Forces who gave me opportunity to get my entire graduate education in the Faculty of Engineering at Boğaziçi University.

ATMOSPHERIC EFFECTS ON PROPAGATION
DUE TO DIFFERENT PARTICLE SHAPES

ABSTRACT

The purpose of this thesis is to determine the effects of atmospheric particles on electromagnetic wave propagation. Especially, the atmospheric conditions are very important at the millimetric waves.

The scattering and absorption cross-sections are calculated for single particle, and then the same process is generalized for an arbitrarily oriented single particle in the atmosphere by means of Euler Angle Rotation.

After calculation of scattering and absorption cross-section, in general, the expressions of attenuation of electromagnetic waves are computerized as a function of rainfall rate. It is shown that precipitation affects the millimetric waves very much. We have to determine the effects of atmosphere clearly to help engineer design more realistic system.

PROPAGASYONDA DEĞİŞİK PARÇACIK ŞEKİLLERİNDEN
DOĞAN ATMOSFERİK ETKİLER

ÖZET

Bu tezin amacı atmosferin elektromagnetik dalgalar üzerindeki etkilerini belirlemektir. Özellikle, atmosfer şartları milimetrik dalgalarda çok önemlidir.

Elektromagnetik dalgaların saçılma ve yutulması tek parçacık için hesaplandı ve daha sonra Euler açısı dönüşümü yardımıyla uzaya rasgele yerleştirilmiş bir parçacık için aynı işlem yapıldı.

Parçacıkta saçılma ve yutulmaya neden olan alanı bulduktan sonra en genel anlamda elektromagnetik dalgaların zayıflaması saatteki yağın yağmurun fonksiyonu olarak kompütürize edildi. Yağmurun milimetrik dalgaları daha çok etkilediği ortadadır. Mühendisin daha gerçekçi sistem tasarlamasına yardımcı olmak için atmosferin etkilerini belirlemek zorundayız.

TABLE OF CONTENTS

	<u>Pages</u>
ABSTRACT.....	iv
ÖZET.....	v
TABLE OF CONTENTS.....	vi
LIST OF FIGURES.....	ix
LIST OF SYMBOLS.....	xi
LIST OF TABLES	
CHAPTER I. INTRODUCTION.....	1
CHAPTER II. ATMOSPHERE AND MILLIMETER WAVES.....	5
2.1. The usage of millimeter waves.....	5
2.2. Causes of attenuation in Atmosphere.....	7
2.2.1. Refractive index.....	7
2.2.2. Attenuation by atmospheric gases....	11
2.2.3. Attenuation by clouds and precipitation.....	13
2.2.4. Attenuation for different wavelengths.....	18
CHAPTER III. SCATTERING AND ABSORPTION BY PARTICLE.....	21
3.1. Introduction.....	21
3.2. Mie scattering theory.....	23
3.3. Rayleigh approximation.....	26
3.4. Rayleigh-Gans approximation.....	28

	<u>Pages</u>
3.5. Scattering and absorption of a plane wave by a single particle.....	32
3.5.1. Basic scattering formulation...	32
3.5.2. Calculation of scattering and absorption cross-sections.....	35
3.5.3. Special cases.....	43
CHAPTER IV. CALCULATION OF AMPLITUDE FUNCTIONS.....	44
4.1. Scattering from arbitrarily oriented single particle.....	44
4.2. Amplitude functions.....	52
4.2.1. Calculation of horizontal amplitude function.....	52
4.2.2. Calculation of vertical amplitude function.....	54
4.3. Cross-Section formulation.....	55
4.4. Drop-Size distribution.....	57
4.5. Attenuation due to different shapes...	59
CHAPTER V. APPLICATIONS.....	61
5.1. The computer program.....	61
5.2. Numerical results and discussion.....	75

	<u>Pages</u>
CONCLUSION.....	83
REFERENCES.....	84
APPENDIX : CALCULATION OF VOLUME INTEGRAL.....	92

LIST OF FIGURES

FIGURE 2.1. Attenuation at millimeter waves

FIGURE 2.2. Attenuation v.s. Raindrop diameter

FIGURE 2.3. Attenuation v.s. Rainfall rate

FIGURE 2.4. Theoretical attenuation v.s. Rainfall rate

FIGURE 2.5. Attenuation by clouds and fog as a function
of wavelength

FIGURE 3.1. Geometry for R.G approximation

FIGURE 3.2. Geometry for scattering

FIGURE 3.3. Scattering from ellipsoid

FIGURE 4.1. Rotated dielectric ellipsoid

FIGURE 5.1. Normalized cross-section vs. raindrop diameter

FIGURE 5.2. Normalized cross-section vs. raindrop diameter

FIGURE 5.3. Normalized cross-section vs. raindrop diameter

FIGURE 5.4. Attenuation v.s Rainfall rate

FIGURE 5.5. Attenuation v.s Rainfall rate

FIGURE 5.6. Attenuation vs. wavelength

LIST OF SYMBOLS

v = Velocity of the wave

ϵ_1 = Permittivity of the medium (ϵ_0 for free space)

μ_1 = Permeability of the medium (μ_0 for free space)

m = Refractive index of atmosphere

(m' is real whereas m'' is the complex part of m)

M = Index of refraction (alternative from)

A = Attenuation

\vec{S}

S = Poyting vector

Q_{sc} = Scattering cross section, σ_s

Q_{ab} = Absorption cross section, σ_a

α = Size parameter = $k \frac{D}{2}$ (D =diameter of particle)

k = Propagation constant

$F(o,i)$ = Scattering amplitude

F_{VV} = Vertical scattering amplitude

F_{HH} = Horizontal scattering amplitude

CHAPTER I

INTRODUCTION

The electromagnetic waves of millimeter wavelengths are now utilized for communication purposes because of their large available bandwidths. Millimeter waves have also some particular advantages such as the use of high gain and high resolution antennas with moderate size and compact components.

Considerable interest has been demonstrated recently in millimeter waves for applications in communication, Radio astronomy, and high resolution radar.

Radar meteorologists have been unable to observe certain types of clouds at centimeter wavelengths and have noted that shorter wavelengths, millimeter wavelength, would be desirable. In many cases, millimeter waves may be an optimum choice for radar meteorology, especially where high resolution is desired.

It is known that millimeter waves are sensitive to rain, fog, and cloud droplets. The most important in-

fluence of the atmosphere on propagation above 10 GHz is attenuation by precipitation. The well-known Mie theory is the basis for models of attenuation. Millimeter waves are attenuated by atmospheric absorption, refraction and scattering. The degree of attenuation is related in a complex way to meteorological conditions along the path of propagation.

This thesis has five chapters. In the first chapter, introduction is given.

The second chapter contains information about millimeter waves and atmosphere and also a complete simplified analysis of millimeter waves attenuation in atmosphere due to different atmospheric conditions.

The third chapter includes a mathematical representation of scattering and absorption by a small particle. Under-quasi-static approximation a sort of generalization of Rayleigh-Gans is being obtained. In addition scattering by an ellipsoid, same is used to

obtain results of circular disks, thin cylinder and sphere. As a special case, our result converges the result in the literature.

In the fourth chapter of this thesis a complete simplified analysis of electromagnetic waves attenuation in atmosphere due to different shapes such as circular disks, thin cylinder, sphere and so on, is given. On the other hand, the single scatterer contrary to chapter III is arbitrarily oriented in the atmosphere and scattering phenomena is generalized. Finally we prove that results for scatterer which is oriented in the origin of the cartesian system are special case of the arbitrarily oriented scatterer.

The fifth chapter of this work contains the numerical results, discussion and computer program. The numerical routines and results are obtained for circular disk, thin cylinder and sphere. Here we

compare our results with experimental results and agreement was found.

CHAPTER II

ATMOSPHERE AND MILLIMETER WAVES

2.1. THE USAGE OF MILLIMETER WAVES

The term millimeter waves generally refers to the electromagnetic spectrum between 30 and 300 GHz (Giga), corresponding to wavelengths of 10 to 1mm. Therefore, the millimeter wave spectrum lies between the microwaves and infrared portions of the electromagnetic spectrum. The Institute of Electrical and Electronics Engineers in the United States identifies the millimeter wave region as lying between 40 and 300 GHz.

The electromagnetic spectrum up to 10 GHz is becoming overcrowded. The earth-space communication requirements have to exceed the electromagnetic spectrum. That is why we have to consider the feasibility of using the millimeter wave region. That is, the millimeter waves spectra with their large available bandwidths must be considered. High gain and high resolution antennas, to-

gether with moderate size and compact components some of the particular advantages of this extended range of the spectrum.

Millimeter wavelengths are utilized for communication purposes especially as space-to-space links.

The main limitation for the use of millimeter waves is the high atmospheric attenuation.

2.2. CAUSES OF ATTENUATION IN ATMOSPHERE

It is well-known that the atmospheric propagation of millimeter waves is strongly affected by certain meteorological phenomena. In general, the attenuation of radio waves of centimeter or millimeter wavelengths in a clear atmosphere near ground level is negligible for most practical purposes.

Millimeter waves are attenuated by atmospheric absorption, refraction and scattering. The degree of attenuation is related in a complex way to meteorological conditions along the path of propagation.

Attenuation is the reduction of intensity of electromagnetic wave along its path. Formulation for attenuation is given in the next chapter.

2.2.1. REFRACTIVE INDEX

Using Maxwell's equations, one can show that in a homogeneous medium the velocity of a wave is given by

$$v = \frac{1}{\sqrt{\epsilon_1 \mu_1}} \quad \dots\dots(2.1)$$

where ϵ_1 is the permittivity of the medium and μ_1 is its permeability. In free space the speed of the wave is equal to the speed of light and is given by

$$c = \frac{1}{\sqrt{\epsilon_0 \mu_0}} \quad \dots\dots(2.2)$$

where ϵ_0 is the permittivity of the free space and μ_0 is its permeability. For most purposes, the speed of propagation of an electromagnetic wave may be considered to be constant and equal to the speed of light in free space, 3×10^8 m/sec.

In the optics, the index of refraction is defined as

$$m = \frac{c}{v} \quad \dots\dots(2.3)$$

or

$$m^2 = \epsilon \mu \quad \dots\dots(2.4)$$

where the dielectric constant of a medium $\epsilon = \epsilon_1 / \epsilon_0$, and permeability $\mu = \mu_1 / \mu_0$ for most practical cases, permittivity $\mu = 1$, then

$$m^2 = \epsilon \dots\dots(2.5)$$

Since ϵ usually exceeds unity, the index of refraction also exceeds unity.

In most general form, the refraction index is a complex function.

That is,

$$m = m' - jm'' \dots\dots(2.6)$$

where the imaginer part m'' is equal to zero in a perfect dielectric and is associated with the absorption of the medium. While we are dealing with the scattering and absorption calculation, of course, it will be quite important.

For dry air, the index of refraction m , is given by

$$(m - 1) \times 10^6 = K_1 \frac{P}{T} \dots\dots(2.7)$$

where P is air pressure in millibars, T is temperature in degrees Kelvin, and K_1 is a constant which has a value of 77.6. Left side of equ (2.7) is so called radio refractivity and $(m-1) \times 10^6$ is referred to as "N units".

While the height of atmosphere is increasing, the value of refractive index decreases. That is why atmosphere is assumed to be stratified. The stratified atmosphere causes the bending of electromagnetic wave. This bending is called refraction. The index of refraction of the earth's atmosphere at microwave frequencies is given by/1/

$$M = (m-1) \times 10^6 = 77.6 \frac{P}{T} + 3.73 \times 10^5 \frac{e}{T^3} \dots\dots(2.8)$$

where m = index of refraction

M = index of refraction (alternative form)

P = air pressure

T = temperature , K

e = pressure of water vapor (in millibars)

Standard atmosphere is assumed to consist of horizontally stratified layers. For standard atmosphere, P and e decrease rapidly with height of the atmosphere and T decreases slowly. Therefore, m decreases with height and a wave passing from a lower to upper layer is bend downward.

For dry atmosphere refractive index is almost constant. Refractive effects vary widely with meteorolo-

gical conditions and for some abnormal cases the wave bends sharply downward (superrefraction), upward (subrefraction), or becomes trapped (ducting). A loss in signal due to refraction should be distinguished from attenuation by absorption or multiple scattering.

2.2.2. ATTENUATION BY ATMOSPHERIC GASES

The atmospheric gases that attenuate millimeter waves (as absorption process) are water vapor and oxygen. As shown in Fig.2.1, atmospheric attenuation is a function of wavelength for typical clear-sky conditions. Water vapor and oxygen molecules have permanent electric and magnetic dipole moments. If they are excited by an electromagnetic wave, they absorb discrete amounts of energy from wave and raised to a higher energy level. While they are coming back to a lower level, they are radiating their energy isotropically. That is why they cause an attenuation of the incident wave.

Water vapor has resonances at frequency of 22 GHz (wavelength ≈ 1.35 cm) and also at frequency of about 180 GHz (wavelength ≈ 1.6 mm). In the region of 60 GHz

(wavelength $\approx 5\text{mm}$) and 120 GHz (wavelength $\approx 2.5\text{mm}$) Oxygen resonance (takes place).

The shapes of the water vapor resonance curves are dependent on atmospheric temperature, pressure and pressure of water vapor whereas in the oxygen case, shapes are functions of atmospheric temperature and pressure.

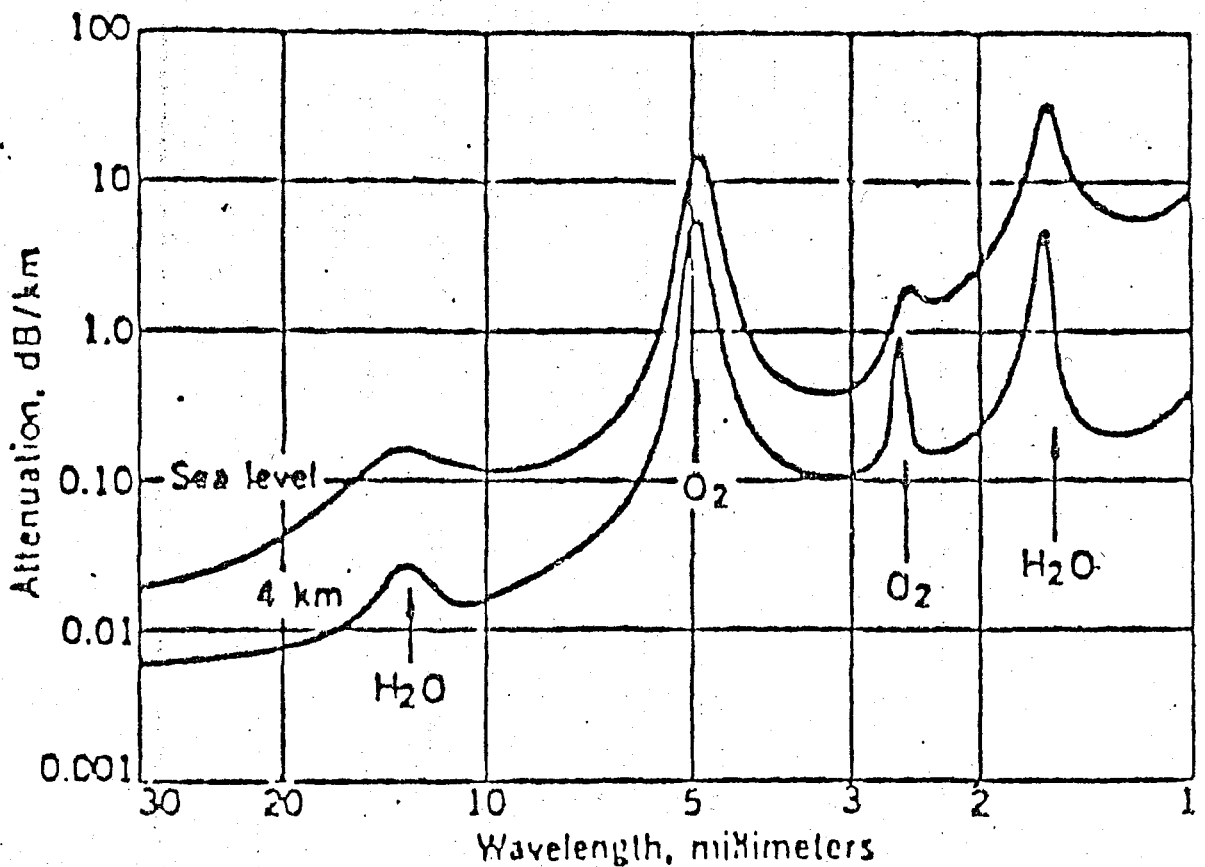


Fig.2.1. Attenuation at millimeter wavelengths/3/

2.2.3. ATTENUATION BY CLOUDS AND PRECIPITATION

Clouds and precipitation attenuate electromagnetic waves. Equation for absorption and scattering have been derived by Gustav Mie (1908). Mie's work has been restated by Straton (1941), Golstein (1946), Kerr (1951) and by Van de Hulst (1957). Mie theory ^{*} treats spherical particles of any material in a nonabsorbing medium.

If the droplets are very small, i.e. diameter of droplet \ll wavelength, the Rayleigh approximation can be applied. Cloud droplets are generally less than 100 μm in diameter.

Ice clouds, like cloud droplets, causes absorption rather than scattering. Attenuation caused by rain has been calculated for spherical shapes from Mie theory (see ref.1). In Fig.2.2, for two different wavelengths, relative Mie attenuation is plotted as a function of drop diameter .

* Detailed information is given later

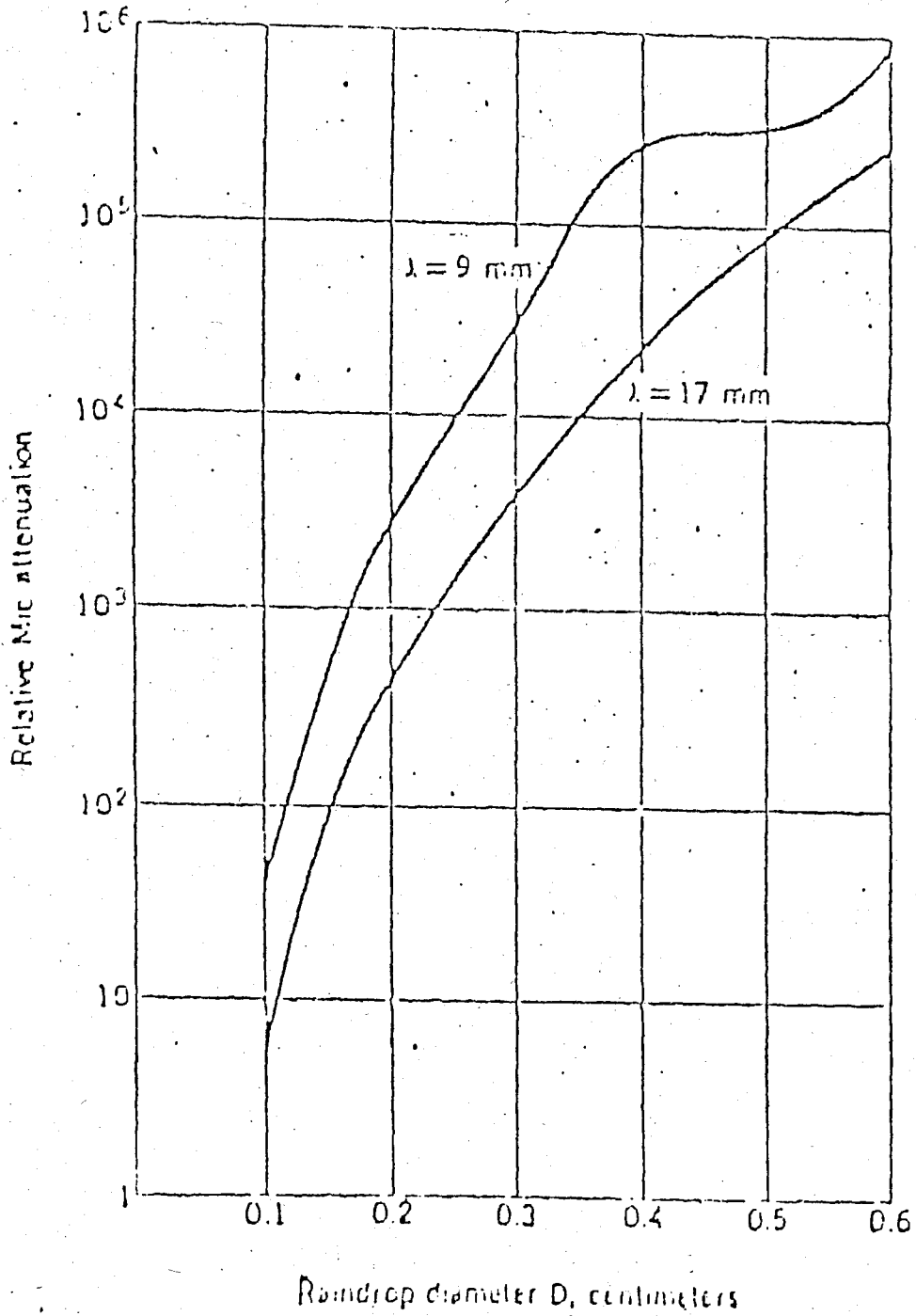


Fig.2.2. Raindrop diameter vs. Relative Mie attenuation /1/.

Attenuation increases rapidly with drop size. Attenuation for $\lambda=9\text{mm}$ is greater than attenuation for $\lambda=17\text{mm}$.

As stated in previous section, in the millimetric wave region, attenuation is very high.

It is possible that we can estimate attenuation as a function of rainfall rate, (see Fig.2.3). It has been found that attenuation due to rain is approximately proportional that to the number of droplets per unit volume. Attenuation versus number of droplets is formulated in the next chapter.

Dry snow and hail causes low attenuation compared with rain, whereas wet snow creates same amount of attenuation like water spheres of the same volume.

Attenuation by rain was computed by Medhurst /2/. Results are shown in Fig.2.4 for $\lambda=1,3$ and 5mm and also $1,3$ and 10cm . When the data are plotted as in Fig.2.4, the points for a given wavelength are nearly colinear. Strait lines have been added for convenience in interpolation.

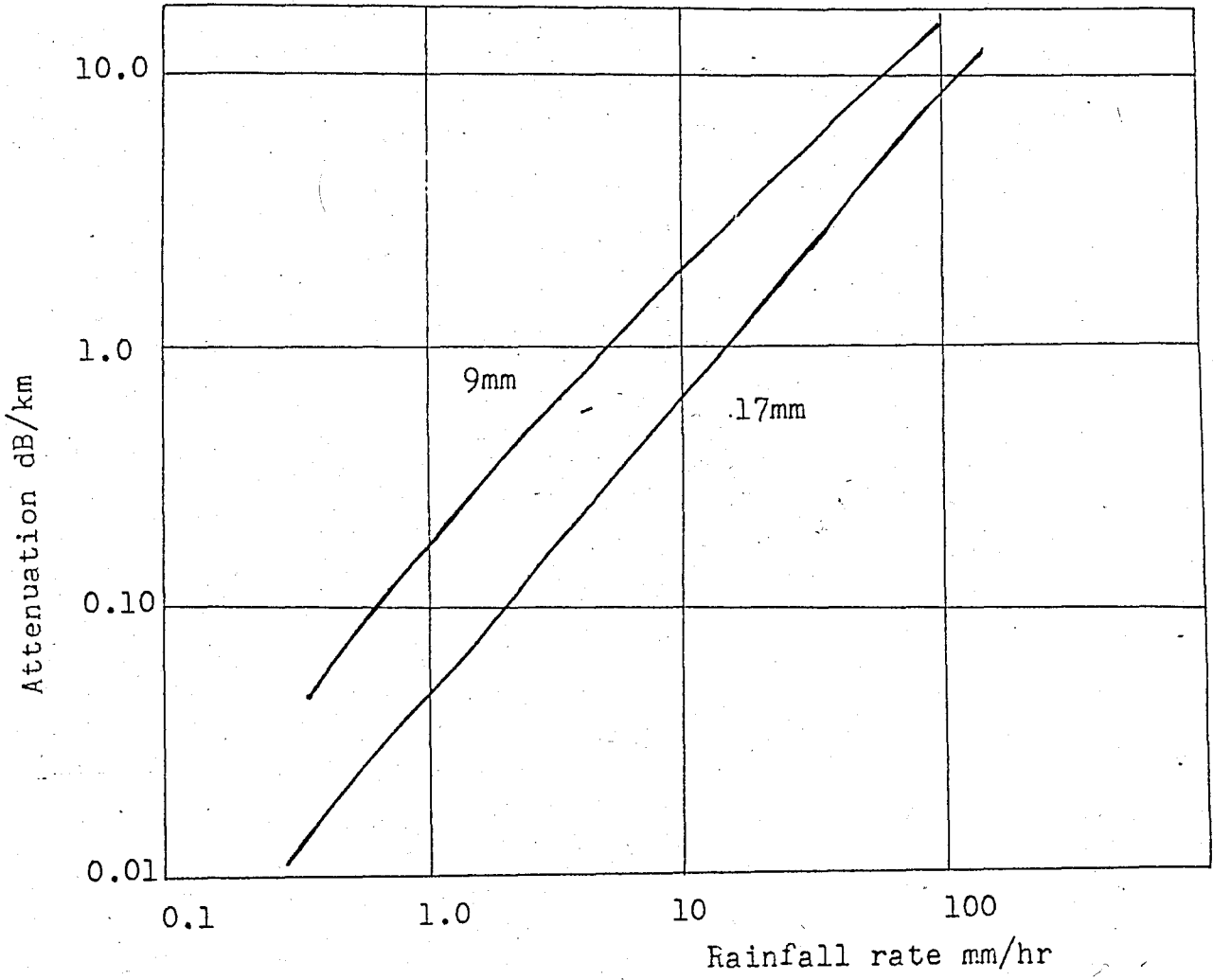


Fig.2.3. Attenuation v.s Rainfall rate/l/.

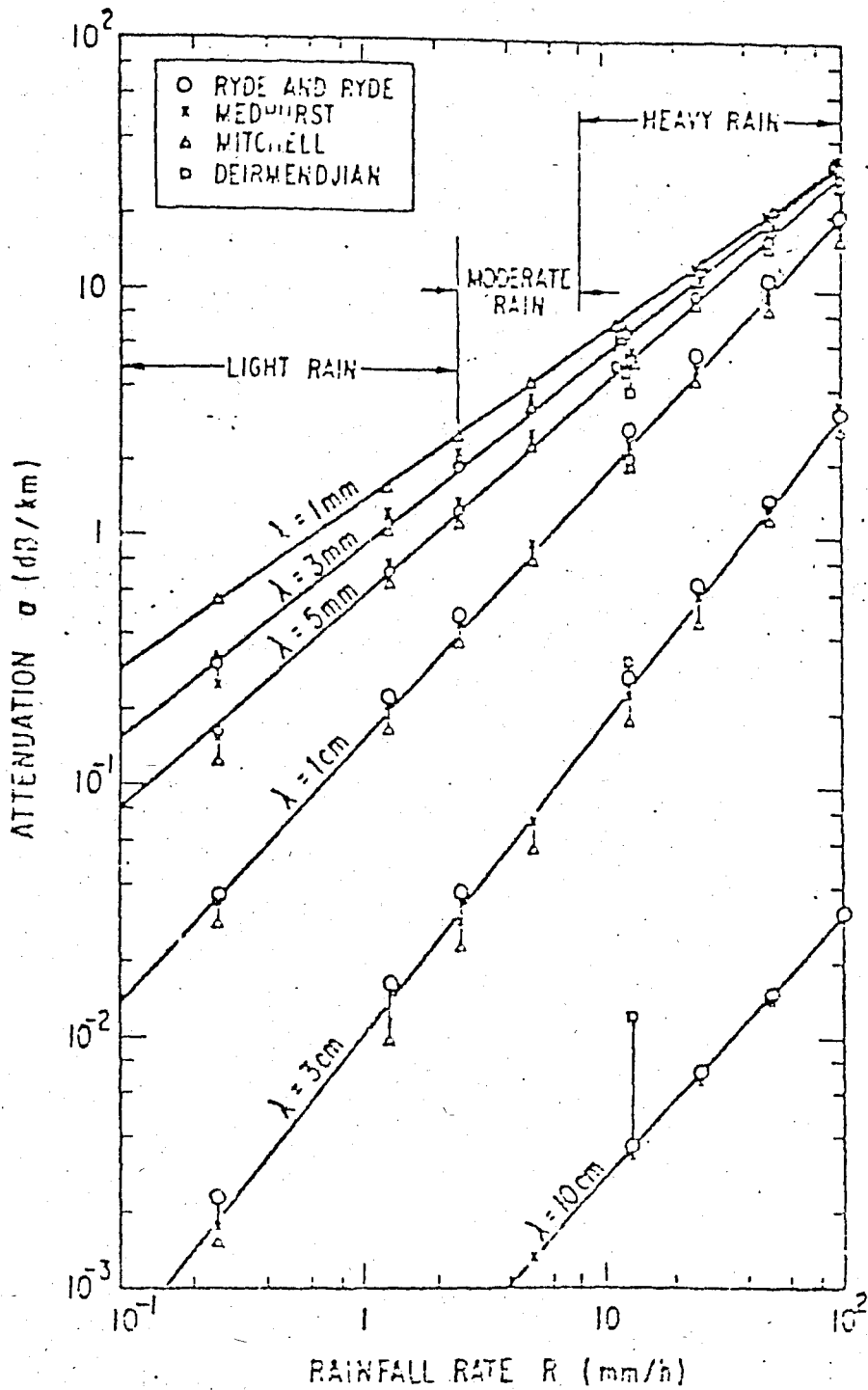


Fig.2.4. Attenuation vs. Rainfall rate /3/.

2.2.4. ATTENUATION FOR DIFFERENT WAVELENGTHS

It is known that the attenuation of electromagnetic waves by hydrometeors in the atmosphere may result from both absorption and scattering, depending on the size and shapes.

Mie scattering theory gives information about cross-sections of particles. When the particles are small with respect to wavelength (Rayleigh approximation), attenuation is considerably simplified for those small particles.

In the case of clouds and fog at millimeter wavelength, the attenuation in decibels per unit length is given by /3/.

$$A = \frac{4.343 \pi^2 \text{Im}(-K)}{\lambda} \int_{\text{Volume}} D^3 N(D) dD \quad \dots(2.9)$$

Where $N(D)dD$ is the number of drops per cubic metre Mitchell's report takes the volume integral as just $6/\pi$ times the total volume. He assumed that the density of particles is 1g/cm^3 , and defined attenuation as

$$A(\text{dB/km}) = 81.86 \frac{\text{Im}(-K)}{\lambda} M \dots\dots(2.10)$$

Where Im= imaginar part of (-K)

$$K = (m^2 - 1) / (m^2 + 2)$$

M= the liquid water content in g/m³. λ is in mm.

Plots of Attenuation/M for clouds and fog as a function of wavelength at temperatures of 0°C and 20°C are give in Fig (2.5).

The attenuation in dB/km/g/m³ varies approxi- mately as λ⁻². He also pointed out that the validity of Rayleigh approximations was dependent on both dia- meter, D, and Wavelength, λ.

Fig.2.5 was obtained for sphere. In our work, attenuation is plotted as a function of rainfall rate not only for sphere for different shapes as well. Our result approaches previous results. Attenuation for dif- ferent shapes is given in chapter IV.

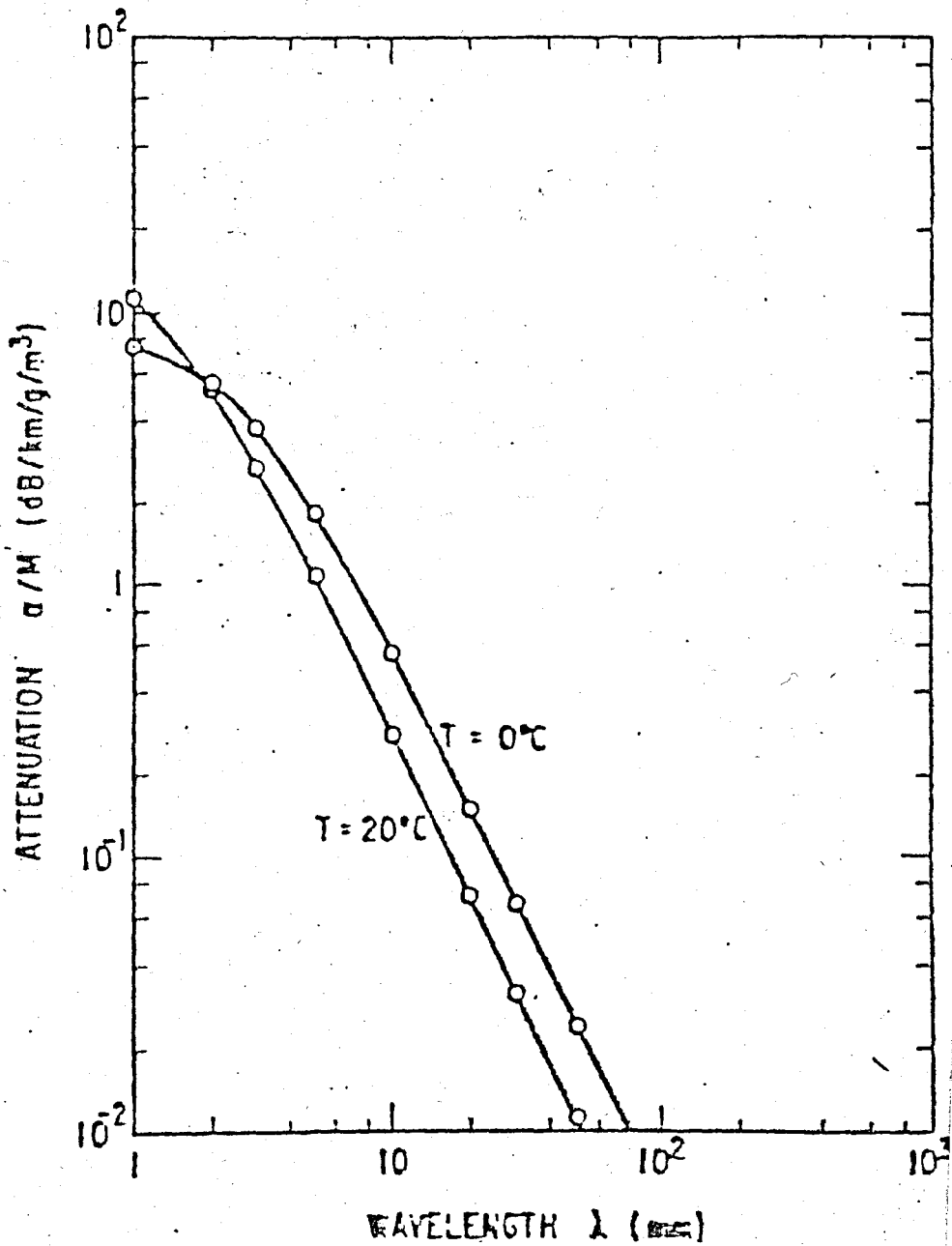


Fig. 2.5 Attenuation by clouds and fog as a function of wavelength. /3/.

CHAPTER III

SCATTERING AND ABSORPTION BY PARTICLE

3.1. INTRODUCTION

The scattering of a plane wave by a dielectric sphere was described by G. Mie in 1908. Mie did not use any approximations. That is why Mie solutions are very complicated. Many authors have pointed out that certain approximations would be possible in the scattering formulation.

Rayleigh developed the full formulas for sphere in his paper in 1910. Further contributions were made by Debye in 1915.

In 1925, Gans rederived the scattering formula for a homogeneous sphere. In order to distinguish it from Rayleigh scattering, which is restricted to particles small compared to the wavelength, this approach has generally been termed Rayleigh-Gans scattering. Actually Gans' contribution to this method was hardly significant and it seems more appropriate to call it Rayleigh-Debye scattering.

A modification of the Rayleigh-Debye (or Rayleigh-Gans) approximation was given by Sihimizu /20/. Sihimizu's paper includes the information of the refractive index of scatterers. He took the radius of the scattering sphere to be the product of refractive index, m , and the radius of scatterer rather than to be radius alone. One then carries out the standard Rayleigh-Gans calculation. Just the same, in the unmodified Rayleigh-Gans approximation, the scattering results are independent of refractive index, m . Sihimizu points out that this approach yields considerably better agreement (with Mie theory) for the angular positions of successive extrema in the scattering.

This chapter includes information about Mie scattering theory, Rayleigh approximation, Rayleigh-Gans approximation, calculation of scattering cross-section, absorption cross-section and also Ishumaru /4/ result as a special case

3.2. MIE SCATTERING THEORY

The exact solution of the scattering of a plane wave by an isotropic, homogeneous sphere was obtained by Mie in 1908, and is usually called the Mie theory.

Mie separated the field equations in spherical coordinates into two groups—one transverse magnetic and the other transverse electric. Matching the boundary conditions at the surface of the sphere, he obtained the cross-sections of a spherical particle.

The scattering cross-section, Q_{sc} is the area which, when multiplied by the incident intensity, gives the total power scattered by the particle; Q_{ab} , the absorption cross-section, is the area which, when multiplied by the incident intensity, gives the power dissipated as internal heat in the particle. The total cross-section Q_t , is the area which, when multiplied by the incident power intensity, gives the total power taken from the incident radio wave, of course, Q_t is equal to the sum of Q_{sc} and Q_{ab} .

In order to evaluate these cross-sections, Mie consider a concentric sphere outside the scattering particle whose radius is large compared to that of the particle. Here the field is the sum of the incident and scattered fields, and the energy flow is found in the usual way from the real part of the time average of Poynting's vector,

$$S = (E_i + E_s) \times (H_i^* + H_s^*) \dots\dots\dots(3.1)$$

The integral of this over the large concentric spherical surface gives the total outward flow of energy.

When the above vector product is expanded in terms of the scalar components of the field vectors and the integration performed, the result can be,

$$I = \text{Re} \int_0^\pi \int_0^{2\pi} \frac{1}{2} (E_{i\theta} H_{i\phi}^* - E_{i\phi} H_{i\theta}^*) r^2 \sin\theta d\theta d\phi \dots\dots\dots(3.2)$$

$$II = \text{Re} \int_0^\pi \int_0^{2\pi} \frac{1}{2} (E_{s\theta} H_{i\phi}^* + E_{i\theta} H_{s\phi}^* - E_{s\phi} H_{i\theta}^* - E_{i\phi} H_{s\theta}^*)$$

$$r^2 \sin\theta d\theta d\phi \dots\dots\dots(3.3)$$

$$III = \operatorname{Re} \int_0^\pi \int_0^{2\pi} \frac{1}{2} (E_{se} H_{s\theta}^* - E_{s\theta} H_{se}^*) r^2 \sin\theta d\theta d\phi \quad \dots\dots(3.4)$$

where the components $E_{ie}, H_{i\theta}^*, E_{se}, E_{s\theta}, E_{i\theta}, H_{se}^*, H_{s\theta}^*, H_{ie}^*$ are field components which are in the spherical coordinates. (*) represents complex conjugate.

The first integral measures the net overflow of energy in the unperturbed incident wave and gives zero as long as the medium is a perfect dielectric (conductivity=0). The third integral which shows the energy of the scattered field is scattering cross-section. Obviously, if the energy is to be conserved, the second integral must be negative. This is because the net energy flow must be negative absorption cross-section, since by virtue of the absorption within it, the particle acts as an energy sink of this magnitude.

These integrals have been evaluated by G.Mie. He expressed them as,

$$Q_{ab} = \frac{\lambda^2}{2\pi} (-\operatorname{Re}) \sum_{n=1}^{\infty} (2n+1)(a_n + b_n) \quad \dots\dots(3.5)$$

$$Q_{sc} = \frac{\lambda^2}{2\pi} \sum_{n=1}^{\infty} (2n+1) (|a_n|^2 + |b_n|^2) \dots\dots\dots(3.6)$$

where a_n and b_n are spherical bessel functions of order n , and they are given in terms of the complex index of refraction, the radius of sphere a , and wavelength of the wave, λ .

3.3. RAYLEIGH APROXIMATION

Rayleigh points out that the cross-section is inversely proportional to the fourth power of the wavelength and directly proportional to the square of the volume of the scatterer. These two characteristics of a small (diameter \ll wavelength) scatterer were derived by Rayleigh.

As restated in Ref /5/, Mie scattering coefficients have been carried out to powers of 10 powers of α (size parameter = $2\pi a/\lambda$, a is radius of scatterer) for real part; the imaginary part of scattering coefficients (a_n and b_n , scattering coeff.) also has been

carried out to the powers of 7 (Powerseries expansion in α in the same reference). After deriving the series solution, equations for Q_{sc} and Q_{ab} were evaluated in many textbooks. The series expansion becomes simple equation if the diameter of scatterer is much less than the wavelength, then for Rayleigh region

$$Q_{sc} = \frac{8}{3} \alpha^4 \left| \frac{m^2 - 1}{m^2 + 2} \right| \dots\dots\dots(3.7)$$

and

$$Q_{ab} = \text{Im} \left\{ -4 \alpha \left(\frac{m^2 - 1}{m^2 + 1} \right) \right\} \dots\dots\dots(3.8)$$

As seen equ's (3.7) and (3.8), if the particles are much smaller than a wavelength, a single term in the Mie series dominates, and the quantities Q_{ab} and Q_{sc} reduces to equ's (3.7) and (3.8). These two equations are so called "Rayleigh expressions" In other words, if $\alpha \ll 1$, we can easily obtain Rayleigh approximations of Q_{ab} and Q_{sc} , from eqs (3.5) and (3.6)

3.4. RAYLEIGH-GANS APPROXIMATION

Rayleigh developed the theory of scattering by small particles and also presented an approximate theory for particles of any shape and size having a small relative index of refraction. Further contributions were made by Debye in 1915. Ten years later, Gans rederived the scattering formulas for a homogenous sphere.

The fundamental approximation in the Rayleigh-Gans approach is that the "phase shift" corresponding to any point in the particle be negligible, i.e., that

$$2ka(m-1) \ll 1 \quad \dots\dots\dots(3.9)$$

where a is the longest dimension through the particle. That is why neither the particle size nor the relative refractive index can become too large.

For incident radiation polarised perpendicular to the scattering plane, the amplitude function for each volume element is given by /5/

$$dS_1(\theta) = j \frac{3}{4\pi} \alpha^3 \left(\frac{m^2 - 1}{m^2 + 2} \right) e^{j\mathbf{s} \cdot \mathbf{r}} dV \quad \dots\dots\dots(3.10)$$

Where $e^{j\delta}$ relates the phase of each elemental wavelet at the position of the observer to a common reference such as the plane P.

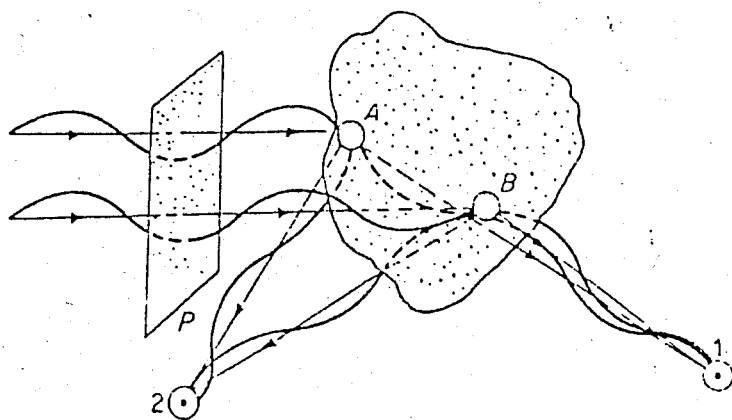


Fig .3.1. Geometry for approximation

At observation points 1 and 2, this approximation says that the phase of each wavelet (as seen in Fig.3.1) is determined only by the position of each volume element. Whereas the phase of each wavelet is independent of the material properties of the particle. This is an important consequence of Rayleigh-Gans approximation.

If m sufficiently close unity, one can write

$$S_1(\theta) = j \frac{3}{4\pi} \alpha^3 \left(\frac{m^2 - 1}{m^2 + 2} \right) \int e^{j\delta} dV \dots\dots(3.11)$$

and finally, $S_1(\theta)$, amplitude function be comes

$$S_1(\theta) = \frac{j}{2\pi} \alpha^3 (m-1) \int e^{j\delta} dV \dots\dots(3.12)$$

If m is real, the scattered intensity is defined as

$$I_1 = (k^4 V^2 / 4\pi^2 r^2) (m-1)^2 P(\theta) \dots\dots(3.13)$$

where

$$P(\theta) = \frac{1}{V^2} \left| \int e^{j\delta} dV \right|^2$$

$P(\theta)$ is so called the form factor.

If the incident wave is polarised parallel to the scattering plane, the scattered wave is obtained as for Rayleigh scatterer, then

$$I_2 = (k^4 V^2 / 4\pi^2 r^2) (m-1)^2 \cos^2\theta P(\theta) \dots\dots(3.14)$$

This assumes no depolarization of the scattered radiation. There is no phase retardation between the perpendicular and parallel components.

The part of each of the above expressions for Rayleigh-Gans approximation is the intensity scattered by a small sphere with volume V . $P(\theta)$ represents the modification of the intensity due to the finite size of the particle and to its deviation from sphericity.

As I mentioned before, Sihimizu modified this approach, he took the radius of the scattering sphere to be refracting sphere to be refractive index multiplied with radius rather than radius alone. Further contributions may be done by developing form factor for different shapes. In next generalised form of the Rayleigh-Gans approach will be obtained.

3.5. SCATTERING AND ABSORPTION OF A PLANE WAVE BY A SINGLE PARTICLE

We consider a single particle and examine its scattering and absorption characteristics. We mentioned some of pertinent approximations to the single particle scattering problem in the previous sections.

In this section we consider an ellipsoid whose axis a, b, c coincide with x, y and z at the origin. Then we evaluate internal field, scattering amplitude, scattering and absorption cross sections.

3.5.1. BASIC SCATTERING FORMULATION

A plane electromagnetic wave incident on an arbitrarily oriented dielectric object. The plane wave is assumed to have polarization \underline{q}^0 and to be propagated in the \underline{i} direction, then

$$\underline{E}_{inc}(\underline{r}) = \underline{q} E_0 \exp(jk_0 \underline{i} \cdot \underline{r}) \quad \dots\dots\dots (3.15)$$

where

E_0 = the magnitude of incident wave (V/m)

k_0 = propagation constant

λ = wavelength in the medium

\underline{i} = unit vector in the direction of wave propagation

\underline{q} = vector in the direction of its polarization

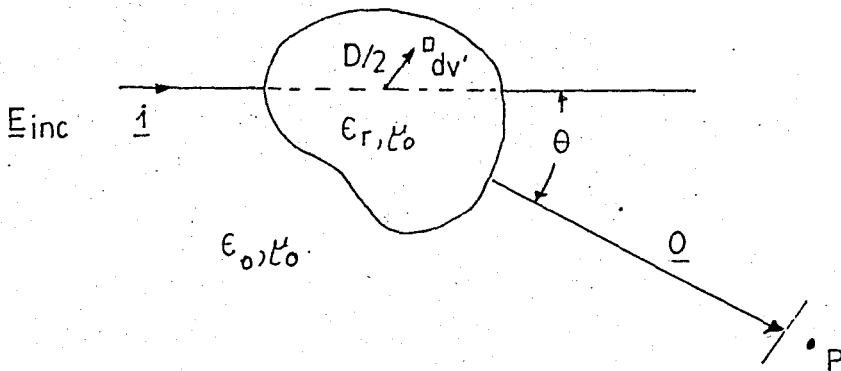


Fig 3.2 Geometry of scattering

An isolated scatterer can be electromagnetically characterized by specifying its far field scattering properties via the scattering amplitude, $F(\underline{q}, \underline{i})$. The wave is incident upon a particle (see Fig 3.2) whose dielectric constant has both real and imaginary parts. That is, the particle may be lossy and inhomogeneous.

If $R \ll D^2 / \lambda$ (Where D is a diameter of the particle), the field E_s has complicated amplitude and pha-

se variations due to interference between contributions from different parts of the particle and then the observation point is said to be in the near field of the particle. In the case of $R \gg D^2 / \lambda$ the scattered field E_s behaves as a spherical wave and is equal to/4/

$$E_s(\underline{r}) = F(\underline{0}, \underline{i}) \frac{e^{jkR}}{R} \dots\dots\dots(3.16)$$

for the amplitude function,

$$F(\underline{0}, \underline{i}) = \frac{k^2 (\epsilon_r - 1)}{4 \pi} \int_V \left\{ -\underline{0x} [\underline{0x} \underline{E}(\underline{r}')] \right\} dV' \dots(3.17)$$

where $F(\underline{0}, \underline{i})$ indicates the amplitude, phase and polarization of the scattered field.

3.5.2. CALCULATION OF SCATTERING AND ABSORPTION CROSS-SECTIONS

We consider a particle (an ellipsoid) whose surface is given by

$$\frac{x^2}{a^2} + \frac{y^2}{b^2} + \frac{z^2}{c^2} = 1 \quad \dots\dots\dots(3.18)$$

and the incident field E_i has component E_{ix} , E_{iy} in the x,y and z directions, respectively.

For calculation of cross sections let us assume that an ellipsoid's axis coincide with x, y, z axis of the cartesian coordinate system. See Fig 3.3.

$$\underline{0} = \sin\theta_s \cos\phi_s \underline{x}^0 + \sin\theta_s \sin\phi_s \underline{y}^0 + \cos\theta_s \underline{z}^0$$

$$-\underline{i} = \sin\theta_i \cos\phi_i \underline{x}^0 + \sin\theta_i \sin\phi_i \underline{y}^0 + \cos\theta_i \underline{z}^0$$

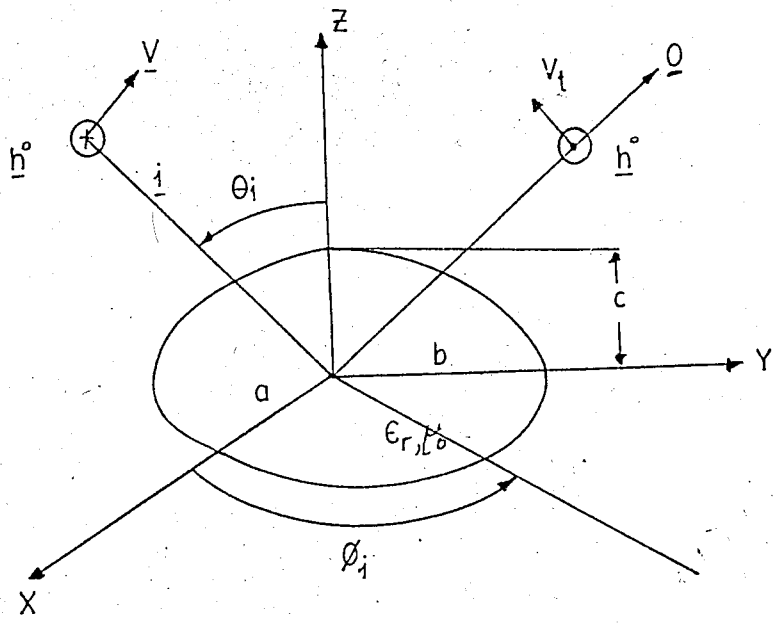


Fig.3.5. Scattering from ellipsoid

We choose $\phi_i = -\frac{\pi}{2}$, then $x^o = h^o$

$$i = \sin\theta_i y^o - \cos\theta_i z^o$$

Field components of the field inside the particle are given by

$$E_x = \frac{E_{ix}}{\left[1 + \frac{abc}{2} (\epsilon_r - 1) A_x\right]} \dots\dots\dots (3.19)$$

$$E_y = \frac{E_{iy}}{\left[1 + \frac{abc}{2} (\epsilon_r - 1) A_y\right]} \dots\dots\dots (3.20)$$

$$E_z = \frac{E_{iz}}{\left[1 + \frac{abc}{2} (\epsilon_r - 1) A_z\right]} \dots\dots\dots(3.21)$$

in which the constants A_x , A_y and A_z are defined as

$$A_x = \int_0^\infty \frac{ds}{(s+a^2) [(s+b^2)(s+c^2)(s+a^2)]^{1/2}} \dots\dots(3.22)$$

$$A_y = \int_0^\infty \frac{ds}{(s+b^2) [(s+b^2)(s+c^2)(s+a^2)]^{1/2}} \dots\dots(3.23)$$

$$A_z = \int_0^\infty \frac{ds}{(s+c^2) [(s+b^2)(s+c^2)(s+a^2)]^{1/2}} \dots\dots(3.24)$$

We assume that the incident field is initially uniform and the internal field within the ellipsoid is also uniform. The depolarising factors L_1 , L_2 and L_3 are defined as

$$L_1 = \frac{abc}{2} A_x \dots\dots(3.25)$$

$$L_2 = \frac{abc}{2} A_y \quad \dots (3.26)$$

$$L_3 = \frac{abc}{3} A_z \quad \dots (3.27)$$

$$\text{and } L_1 + L_2 + L_3 = 1 \quad \dots (3.28)$$

Field inside the ellipsoid is

$$E_y = \frac{E_{iy}}{[1 + L_1(\epsilon_r - 1)]} \quad \dots (3.29)$$

Since $ka \ll 1$, field inside the ellipsoid is constant.

$$\therefore E_x = E_y = \frac{1}{1 + L_1(\epsilon_r - 1)} \quad \dots (3.30)$$

The absorption cross-section is given by /4/

$$Q_{ab} = \int_V k \epsilon_r''(\underline{r}') |\underline{E}(\underline{r}')|^2 dV' \quad \dots (3.31)$$

since ϵ_r'' is constant in our problem, we obtain

$$Q_{ab} = k \epsilon_r'' \int_V |\underline{E}(\underline{r}')|^2 dV' \quad \dots (3.32)$$

where

$\underline{E}(\underline{r}')$ is the electric field inside the ellipsoid,
 ϵ_r'' is the imaginary part of relative dielectric constant of ellipsoid.

by using value of $\underline{E}(\underline{r}')$ for ellipsoid, one can obtain

$$Q_{abh} = \frac{k\epsilon''V}{|1+L_1(\epsilon_r-1)|^2} \dots(3.33)$$

Vertical value of electric field inside the ellipsoid is for incident field of

$$|\underline{E}_v| = (|\underline{E}_y|^2 + |\underline{E}_z|^2)^{1/2} \dots(3.34)$$

where $E_y = \frac{\cos\theta_i}{[1+L_1(\epsilon_r-1)]}$

and $E_z = \frac{\sin\theta_i}{[1+L_3(\epsilon_r-1)]}$

in a similar way, vertical absorption cross section is

$$Q_{abv} = k \epsilon_r'' \int_V |\underline{E}_v|^2 dV'$$

$$\text{or } Q_{abv} = k \epsilon_r'' V \left(\frac{\cos^2 \theta_i}{|1+L_1(\epsilon_r-1)|^2} + \frac{\sin^2 \theta_i}{|1+L_3(\epsilon_r-1)|^2} \right)$$

$$\text{where } L_3 = 1 - 2L_1 \quad \dots (3.35)$$

In order to calculate scattering cross-section, we use definition and then

$$Q_{sc} = \int_{4\pi} Q_d \, d\omega = \int_{4\pi} |F(\underline{0}, \underline{i})|^2 \, d\omega \quad \dots (3.36)$$

$$\text{Let } \underline{E}(\underline{r}') = E_p \underline{p} \text{ and } \underline{p}^0 \in (\underline{h}^0, \underline{v}^0) \quad \dots (3.37)$$

and using equ. (3.17), one can obtain

$$F(\underline{0}, \underline{i}) = \frac{k^2 (\epsilon_r - 1) |E_p|}{4\pi} \left\{ -\underline{0} \times (\underline{0} \times \underline{p}^0) \right\} V \quad \dots (3.38)$$

Note that we can write vector identity in paranthesis as

$$-\underline{0} \times (\underline{0} \times \underline{p}^0) = -[(\underline{0} \underline{p}^0) \underline{0} - (\underline{0} \underline{0}) \underline{p}^0] = \underline{p}^0 - (\underline{0} \underline{p}^0) \underline{0}$$

and also

$$\left| \left[-\underline{0} \times (\underline{0} \times \underline{p}^0) \right] \right| = \sin \chi_p \quad \dots (3.39)$$

where χ is the angle between \underline{p}^0 and $\underline{0}$.

Taking the square of equ.(3.38) one can obtain

$$|\underline{F}(\underline{o}, \underline{i})|^2 = \frac{k^4 |(\epsilon_r - 1)|^2 v^2}{(4\pi)^2} (E_p)^2 \sin^2 \alpha_p \quad \dots (3.40)$$

where $\sin^2 \alpha_p = 1 - (\underline{o} \cdot \underline{p}^0)^2$. Let take $\underline{p} = \underline{h}^0 = \underline{x}^0$ hence $E_p = E_x$ and given by equ.(3.30), now substituting equ.(3.30) into the equ.(3.40), we obtain

$$|\underline{F}_h(\underline{o}, \underline{i})|^2 = \frac{k^4 |\epsilon_r - 1|^2 v^2}{(4\pi)^2 |1 + L_1(\epsilon_r - 1)|^2} \sin^2 \alpha_h \quad \dots (3.41)$$

and then

$$Q_{sch} = \int_{4\pi} |\underline{F}_h|^2 dw = \frac{k^4 |\epsilon_r - 1|^2 v^2}{(4\pi)^2 |1 + L_1(\epsilon_r - 1)|^2} \int_{4\pi} \sin^2 \alpha_h \sin \alpha_h d\alpha_h d\phi \quad \dots (3.42)$$

the value of integral in equ.(3.42) is just equal to $\frac{8\pi}{3}$

$$Q_{sch} = \frac{k^4 v^2}{6\pi} \left| \frac{\epsilon_r - 1}{1 + L_1(\epsilon_r - 1)} \right| \quad \dots (3.43)$$

where

$$V = \frac{4}{3} \pi a^2 c, \quad c = \frac{T}{2}, \quad a = \text{radius}$$

Now, let us take $\underline{p}^0 = \underline{v}^0$, then $E_p = E_v$

$$|\underline{E}_v|^2 = |\underline{E}_y|^2 + |\underline{E}_z|^2 \quad \text{and}$$

$$|\underline{E}_v|^2 = \left\{ \frac{\cos^2 \theta_i}{|1+L_1(\epsilon_r-1)|^2} + \frac{\sin^2 \theta_i}{|1+L_3(\epsilon_r-1)|^2} \right\} \dots (3.44)$$

In a similar way to calculate the vertical scattering amplitude and related vertical cross-section, we can write from equ.(3.40)

$$|F_v(\underline{0}, \underline{i})|^2 = \frac{k^4 |\epsilon_r - 1|^2 v^2}{(4\pi)^2} |\underline{E}_v|^2 \sin^2 \alpha_v \dots (3.45)$$

and then substituting in equ.(3.38)

$$Q_{scv} = \frac{k^4 |\epsilon_r - 1|^2 v^2}{(4\pi)^2} |\underline{E}_v|^2 \int \sin^2 \alpha_v \sin \alpha_v d\alpha_v d\phi \dots (3.46)$$

The value of integral in equ.(3.46) is equal to $\frac{8\pi}{3}$

$$\text{and } Q_{scv} = \frac{k^4 |\epsilon_r - 1|^2 v^2}{6\pi} |\underline{E}_v|^2 \dots (3.47)$$

by substituting value of \underline{E}_v , we obtain

$$Q_{scv} = \frac{k^4 v^2}{6\pi} \left\{ \left| \frac{(\epsilon_r - 1)}{1+L_1(\epsilon_r-1)} \right|^2 \cos^2 \theta_i + \left| \frac{(\epsilon_r - 1)}{1+L_3(\epsilon_r-1)} \right|^2 \sin^2 \theta_i \right\} \dots (3.48)$$

where $L_3 = 1 - 2L_1$. We will generalize this calculation when $\theta \neq 0$ in next chapter.

3.5.3. SPECIAL CASE

In Ref /4/, scattering and absorption cross-sections are given by

$$\sigma_s = \frac{8\pi^3 V^2}{3\lambda^4} \left| \frac{\epsilon_r - 1}{1 + L_1(\epsilon_r - 1)} \right|^2$$

and

$$\sigma_a = k \cdot \epsilon_r'' \left| \frac{1}{1 + L_1(\epsilon_r - 1)} \right|^2 V$$

From the geometry of scattering which is given in section 3.5.2, we can take as a special case, $\theta_i = 0$ then

$$Q_{sc} = Q_{sch} = Q_{scv} = \frac{k^4 V^2}{6\pi} \left| \frac{\epsilon_r - 1}{1 + L_1(\epsilon_r - 1)} \right|^2 \quad \dots (3.49)$$

using $k = 2\pi/\lambda$, equ.(3.49) becomes

$$Q_{sc} = Q_{sch} = Q_{scv} = \frac{8\pi^3 V^2}{3\lambda^4} \left| \frac{\epsilon_r - 1}{1 + L_1(\epsilon_r - 1)} \right|^2 \quad \dots (3.50)$$

Clearly equ.(3.50) is in agreement with Ref /4/

In a similar manner, our result

$$Q_{abh} = Q_{abv} = k \epsilon_r'' V \left| \frac{1}{1 + L_1(\epsilon_r - 1)} \right|^2 \quad \text{is in agree-}$$

ment with Ref/4/

CHAPTER IV

CALCULATION OF AMPLITUDE FUNCTIONS

4.1. SCATTERING FROM ARBITRARILY ORIENTED SINGLE PARTICLE

In this section, previous results are generalised for arbitrarily oriented single particle. We are assuming that ϕ_i is equal to zero degree, then \underline{h}^0 vector coincides with \underline{y}^0 vector.

When the particle is illuminated by a plane wave propagation in the direction \underline{i} , scattering direction \underline{q} can be described by angles θ_s , ϕ_s measured with respect to z and x axes respectively. It is necessary to express variables in the coordinates of reference frame. Let us assume x^{01} , y^{01} , and z^{01} are unit vectors in the primed system, they can be expressed in terms of the reference system using euler angle rotation. We use orthogonal transformation. For this transformation we define a matrix, A , is called the matrix transformation, which can be thought of as an operator.

$$A = \begin{pmatrix} a_{11} & a_{12} & a_{13} \\ a_{21} & a_{22} & a_{23} \\ a_{31} & a_{32} & a_{33} \end{pmatrix} \quad \dots(4.1)$$

Axis acting on the unprimed system and transforming it into the primed system. Matrix A contains nine direction cosines. It is necessary to describe A using some set of three independent parameters. The usual choice of parameters is the euler angles. The goal is to describe the orientation of final rotated system (X_1'', X_2'', X_3'') relative to some initial coordinate system (X_1, X_2, X_3). Three matrices describing these rotations are

$$R_z(\phi) = \begin{pmatrix} \cos\phi & \sin\phi & 0 \\ -\sin\phi & \cos\phi & 0 \\ 0 & 0 & 1 \end{pmatrix} \quad \dots(4.2)$$

$$R_y(\theta) = \begin{pmatrix} \cos\theta & 0 & -\sin\theta \\ 0 & 1 & 0 \\ \sin\theta & 0 & \cos\theta \end{pmatrix} \quad \dots(4.3)$$

$$R_z(\alpha) = \begin{pmatrix} \cos\alpha & \sin\alpha & 0 \\ -\sin\alpha & \cos\alpha & 0 \\ 0 & 0 & 1 \end{pmatrix} \quad \dots(4.4)$$

the total rotation is described as

$$A(\phi, \theta, \alpha) = R_z(\alpha) \cdot R_y(\theta) \cdot R_z(\phi) \quad \dots (4.5)$$

therefore,

$$A(\phi, \theta, \alpha) = \begin{pmatrix} \cos\alpha \cos\theta \cos\phi - \sin\alpha \sin\phi & \cos\alpha \cos\theta \sin\phi + \sin\alpha \cos\phi & \\ -\sin\alpha \cos\theta \cos\phi - \cos\alpha \sin\phi & -\sin\alpha \cos\theta \sin\phi + \cos\alpha \cos\phi & \\ & \sin\theta \cos\phi & \sin\theta \sin\phi \end{pmatrix}$$

$$\begin{pmatrix} -\cos\alpha \sin\theta \\ \sin\alpha \sin\theta \\ \cos\theta \end{pmatrix} \quad \dots (4.6)$$

By using $\underline{x}^{01} = A\underline{x}^0$ we can write

$$z^{01} = \cos\phi \sin\theta \underline{x}^0 + \sin\phi \sin\theta \underline{y}^0 + \cos\theta \underline{z}^0 \quad \dots (4.7)$$

As seen from equ. (4.7), the spherical angles of incident wave θ, ϕ are measured with respect to a polar axis Z and X respectively.

Assuming that θ_i is equal to zero degree and $\underline{h}^0 = \underline{y}^0$, then equ.(4.7) becomes for incident direction

$$\underline{i} = -\sin\theta_i \underline{x}^0 - \cos\theta_i \underline{z}^0 \quad \dots(4.8)$$

On the other hand, from equ.(3.17), we have scattering amplitude for homogeneous and isotropic scatterer,

$$F(\underline{o}, \underline{i}) = \frac{k^2(\epsilon_r - 1)}{4\pi} \int_{V_p} \left\{ -\underline{o} \times \left[\underline{o} \times \underline{E}_o(\underline{r}) \right] \right\} e^{-j\mathbf{k}\underline{r}\cdot\underline{o}} dV' \quad (4.9)$$

In order to calculate scattering amplitude, We have to know the value of field inside the scatterer. Taking the axes of three dimensional scatterer as \underline{r}^0 , $\underline{\theta}^0$, $\underline{\phi}^0$, we obtain the field inside the scatterer as

$$\underline{E} = E_h \underline{h}^0 + E_v \underline{v}^0 = \underline{E}_h + \underline{E}_v \quad \dots(4.10)$$

where

$$\underline{E}_h = E_{hr} \underline{r}^0 + E_{h\theta} \underline{\theta}^0 + E_{h\phi} \underline{\phi}^0 \quad \dots(4.11)$$

and

$$\underline{E}_v = E_{vr} \underline{r}^0 + E_{v\theta} \underline{\theta}^0 + E_{v\phi} \underline{\phi}^0 \quad \dots(4.12)$$

\underline{E}_h shows the field inside the scatterer for horizontal polarization whereas \underline{E}_v indicates the field inside the scatterer for vertical polarisation. In equ's (4.11) and (4.12) vectors \underline{r}^0 , $\underline{\theta}^0$, $\underline{\phi}^0$ can be defined as (check the matrix transform)

$$\underline{r}^0 = \text{Sin}\theta \text{Cos}\phi \underline{x}^0 + \text{Sin}\theta \text{Sin}\phi \underline{y}^0 + \text{Cos}\theta \underline{z}^0$$

$$\underline{\theta}^0 = \text{Cos}\theta \text{Cos}\phi \underline{x}^0 + \text{Cos}\theta \text{Sin}\phi \underline{y}^0 + \text{Sin}\theta \underline{z}^0$$

$$\underline{\phi}^0 = -\text{Sin}\phi \underline{x}^0 + \text{Cos}\phi \underline{y}^0 \quad \dots (4.13)$$

As seen in equ's (4.13), spherical polar unit vectors are in form of the cartesian components.

By using the geometry of Fig 4.1., \underline{r}^0 vector is in coincidence with scattering direction \underline{Q} , we can write

$$\underline{Q} = \text{Sin}\theta_s \text{Cos}\phi \underline{x}^0 + \text{Sin}\theta_s \text{Sin}\phi \underline{y}^0 + \text{Cos}\theta_s \underline{z}^0$$

therefore

$$E_{hr} = E_{ih}(\underline{h}^0 \cdot \underline{r}^0) = E_{ih} \text{Sin}\theta \text{Sin}\phi \quad \dots (4.14)$$

similarly for $E_{ih\theta}$ and $E_{ih\phi}$, we can obtain below relations

$$E_{h\theta} = E_{ih} (h^{\circ} \cdot \theta^{\circ}) = E_{ih} \cos\theta \sin\theta \quad \dots (4.15)$$

and

$$E_{h\phi} = E_{ih} (h^{\circ} \cdot \phi^{\circ}) = E_{ih} \cos\phi \quad \dots (4.16)$$

For vertical components, we can write below relations similarly

$$E_{ivr} = E_{iv} (v^{\circ} \cdot r^{\circ}) = E_{iv} (\sin\theta_i \cos\theta - \cos\theta_i \sin\theta \cos\phi) \quad \dots (4.17)$$

and other components are

$$E_{v\theta} = E_{iv} (v^{\circ} \cdot \theta^{\circ}) = E_{iv} (-\cos\theta_i \cos\theta \cos\phi - \sin\theta_i \sin\theta) \quad \dots (4.18)$$

$$E_{v\phi} = E_{iv} (v^{\circ} \cdot \phi^{\circ}) = E_{iv} (\cos\theta_i \sin\phi) \quad \dots (4.19)$$

As mentioned in chapter III, similarly by using polar components instead of cartesian coordinates components and using geometry in Fig.4.1., equ's (3.19), (3.20), and (3.21) become

$$E_{hr} = \frac{E_{ihr}}{1 + \frac{abc}{2} (\epsilon_r - 1) A_r} \quad \dots (4.20)$$

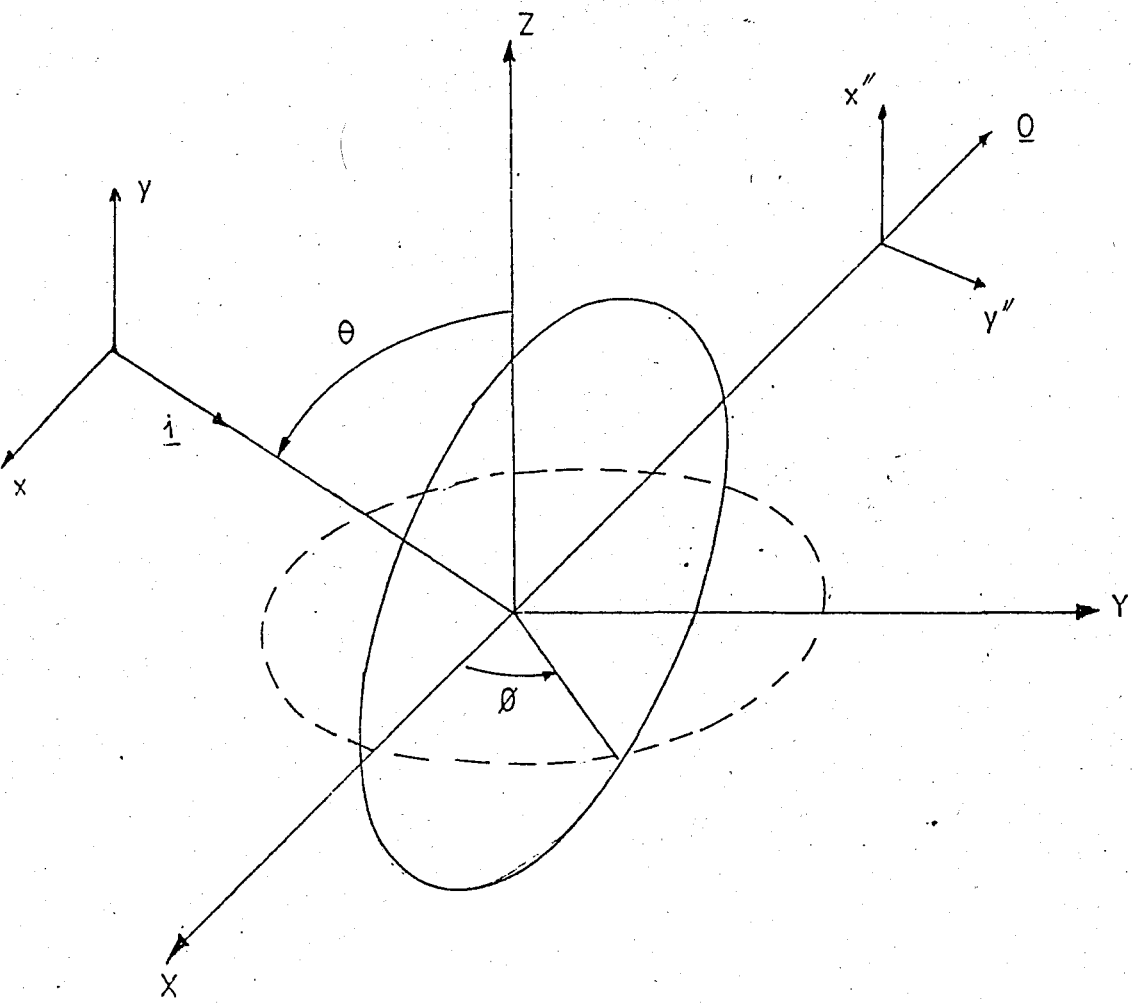


Fig.4.1. Rotated dielectric ellipsoid

$$E_{h\theta} = \frac{E_{ih\theta}}{1 + \frac{abc}{2} (\epsilon_r - 1) A_\theta} \dots (4.21)$$

$$E_{h\phi} = \frac{E_{ih\phi}}{1 + \frac{abc}{2} (\epsilon_r - 1) A_\phi} \dots (4.22)$$

or simply

$$E_{hr} = K_1 E_{ihr} \dots (4.23)$$

$$E_{h\theta} = K_2 E_{ih\theta} \dots (4.24)$$

$$E_{h\phi} = K_3 E_{ih\phi} \dots (4.25)$$

Similarly for vertical polarization we can write

$$E_{vr} = K_1 E_{ivr} \dots (4.26)$$

$$E_{v\theta} = K_2 E_{iv\theta} \dots (4.27)$$

$$E_{v\phi} = K_3 E_{iv\phi} \dots (4.28)$$

where \underline{r}° , $\underline{\theta}^\circ$, $\underline{\phi}^\circ$ are polar spherical unit vectors in the principal frame and

$$K_1 = \frac{1}{1+L_1(\epsilon_r-1)} \quad \dots(4.29)$$

$$K_2 = \frac{1}{1+L_2(\epsilon_r-1)} \quad \dots(4.30)$$

$$K_3 = \frac{1}{1+L_3(\epsilon_r-1)} \quad \dots(4.31)$$

and L_1 , L_2 , L_3 are given by equ's(3.25), (3.26) and (3.27)

By changing the values of L's /6/, We can find internal field for any shape . Now, we can evaluate scattering amplitude since internal field is known.

4.2. AMPLITUDE FUNCTIONS

4.2.1. CALCULATION OF HORIZONTAL AMPLITUDE FUNCTION

Changing the value of L's by using ref /6/, one can obtain the internal field components for different shapes. That is, scattering amplitude is calculable since the internal field is known. We can write for forward direction ($\underline{q} = \underline{i}$) /7/

$$F(\underline{i}, \underline{i}, \underline{h}) = \frac{k^2(m^2-1)}{4\pi} \int_{V_p} \left\{ -\underline{i}x(\underline{i}x\underline{E}_h) \right\} dV' \quad \dots (4.32)$$

or in the explicit form.

$$F(\underline{i}, \underline{i}, \underline{h}) = \frac{k^2(m^2-1)}{4\pi} \int_{V_p} \left\{ -\underline{i}x(\underline{i}x(E_{hr}r^o + E_{he}\theta^o + E_{h\phi}\phi^o)) \right\} dV' \quad \dots (4.33)$$

Horizontal component is obtained by dot product.

$$F_{HH} = F(\underline{i}, \underline{i}, \underline{h}^o) \cdot \underline{h}^o \text{ and using } \underline{i} \cdot \underline{h}^o = 0$$

We can write,

$$F_{HH} = \frac{k^2(m^2-1)}{4\pi} \int_{V_p} \left\{ (\underline{r}^{\circ} \cdot \underline{h}^{\circ}) E_{hr} + (\underline{\theta}^{\circ} \cdot \underline{h}^{\circ}) E_{h\theta} + (\underline{\phi}^{\circ} \cdot \underline{h}^{\circ}) E_{h\phi} \right\} dV' \dots (4.34)$$

where $\underline{r}^{\circ} \cdot \underline{h}^{\circ} = \underline{r}^{\circ} \cdot \underline{y}^{\circ} = \text{Sin}\theta \text{Sin}\phi$

$$\underline{\theta}^{\circ} \cdot \underline{h}^{\circ} = \underline{\theta}^{\circ} \cdot \underline{y}^{\circ} = \text{Cos}\theta \text{Sin}\phi$$

$$\underline{\phi}^{\circ} \cdot \underline{h}^{\circ} = \underline{\phi}^{\circ} \cdot \underline{y}^{\circ} = \text{Cos}\phi \dots (4.35)$$

by substituting (4.35) into (4.34), we obtain

$$F_{HH} = \frac{k^2(m^2-1)}{4\pi} E_{ih} \left(\text{Sin}^2\theta \text{Sin}^2\phi K_1 + \text{Cos}^2\theta \text{Sin}^2\phi K_2 + \text{Cos}^2\phi K_3 \right) \int_{V_p} e^{jk_0 \underline{y} \cdot \underline{x}'} dX' \dots (4.36)$$

The value of integral in eqn.(4.36) is given in appendix.

4.2.2. CALCULATION OF VERTICAL AMPLITUDE FUNCTION

In a similar way, for vertical amplitude, we can write easily /7/

$$F_{VV} = \frac{k^2(m^2-1)}{4\pi} \int_{V_p} dV' \left\{ (\underline{r}^{\circ} \cdot \underline{v}^{\circ}) E_{Vr} + (\underline{\theta}^{\circ} \cdot \underline{v}^{\circ}) E_{V\theta} + (\underline{\phi}^{\circ} \cdot \underline{v}^{\circ}) E_{V\phi} \right. \\ \left. \dots (4.37) \right.$$

where dot products are

$$\underline{r}^{\circ} \cdot \underline{v}^{\circ} = -\cos\theta_i \sin\theta \cos\phi + \sin\theta_i \cos\theta$$

$$\underline{\theta}^{\circ} \cdot \underline{v}^{\circ} = -\cos\theta_i \cos\theta \cos\phi - \sin\theta_i \sin\theta$$

$$\underline{\phi}^{\circ} \cdot \underline{v}^{\circ} = \cos\theta_i \sin\phi \quad \dots (4.38)$$

by substituting equ's (4.38) into the (4.37) one can obtain

$$F_{VV} = \frac{k^2(m^2-1)}{4\pi} E_{iv} \left\{ (-\cos\theta_i \sin\theta \cos\phi + \sin\theta_i \cos\theta)^2 \right. \\ \left. xK_1 + (\cos\theta_i \cos\theta \cos\phi + \sin\theta_i \sin\theta)^2 xK_2 \right. \\ \left. + (\cos\theta_i \sin\phi)^2 xK_3 \right\} \int_{V_p} e^{jk_o \underline{v} \cdot \underline{x}'} dx' \quad \dots (4.39)$$

Scattering amplitudes are calculated for randomly oriented shapes as above.

4.3. CROSS-SECTION FORMULATION

Under quasi-static approximation, internal field of ellipsoid is obtained /7/ as

$$E_{int}(\underline{x}', \underline{q}^0) = E_0 [K_1(\underline{q}^0 \cdot \underline{r}^0) \underline{r}^0 + K_2(\underline{q}^0 \cdot \underline{\theta}^0) \underline{\theta}^0 + K_3(\underline{q}^0 \cdot \underline{\varrho}^0) \underline{\varrho}^0] \quad \dots(4.40)$$

where $\underline{r}^0, \underline{\theta}^0, \underline{\varrho}^0$ and K_1, K_2 and K_3 were defined in section 4.1

We know that internal field determines the value of scattering amplitude. By a straight forward manner, using same definition which is used in (3.5) and by means of same reference, we can obtain easily below formulas,

$$Q_{PP} = \int_V |F(\underline{q}, \underline{i}, \underline{q})|^2 dw \quad \dots(4.41)$$

where dw =solid angle

$$\underline{P} \in \{ \underline{h}^0, \underline{v}^0 \}$$

$$Q_{hh} = \frac{k_o^4 (\epsilon_r - 1) E_o^2}{4\pi} v^2 |K_1(\underline{h}^o \cdot \underline{\theta}^o) + K_2(\underline{h}^o \cdot \underline{\phi}^o) + K_3(\underline{h}^o \cdot \underline{r}^o)|^2$$

....(4.42)

in a similar way,

$$Q_{vv} = \frac{k_o^4 (\epsilon_r - 1) E_o^2}{4\pi} v^2 |K_1(\underline{v}^o \cdot \underline{\theta}^o) + K_2(\underline{v}^o \cdot \underline{\phi}^o) + K_3(\underline{v}^o \cdot \underline{r}^o)|^2$$

....(4.43)

In the geometry of Fig.3.3, ellipsoid is oriented at the origin of the cartesian coordinate system. Whereas, in Fig.4.1, ellipsoid is arbitrarily oriented. If we put $\theta = \phi = 0$ in equations of chapter 4, we find the result of chapter 3. And also, if we put $L_1=L_2=L_3=0.333$ into equations (4.42) and (4.43), one can obtain the results of section special cases of chapter 3. That is, our results are still good agreement with references /3/ and /4/.

4.4. DROP-SIZE DISTRIBUTION

Specific attenuation values were calculated using Mie scattering theory for water spheres at each of 41 frequencies between 1 and 1000 GHz. These values are given in tabular form in /14/. Values for refractive index of water required in the calculations were obtained at temperatures of 20°C, 0°C, and -10°C from equations given by Ray /15/. One can find detailed information about refractive index in this reference.

Four different average drops size distributions were used in the calculations to obtain a range of possible specific attenuation values for each frequency;

1) Laws and Parsons (LP) Distribution /16/

This distribution has been used for many previous calculations. At rain rates below about 35mm/h, this distribution gives reasonable result.

2) Thunderstorm Distribution

This negative exponential distribution measures the average dropsize spectrum in convective rain. It has been used previously for some specific attenuation calculations /17/.

3) "Drizzle" Distribution:

Again this is a negative exponential distribution obtained by fitting the average dropsize spectrum of very light widespread rain, or drizzle composed of small drops /18/

4) Marshall-Palmer Distribution

This negative exponential distribution assumed here/8/. This is fairly good fit for the mean dropsize spectra measured by both Marshall and Palmer and Laws and Parsons. It has been found to be most applicable to widespread rain in continental temperature climates.

Marshall and Palmer distribution is given by

$$n(\bar{a}) = 0.16 e^{-\Lambda \cdot \bar{a}} \quad \dots (4.44)$$

where

$$\Lambda = 82 \cdot R^{-0.21} \quad \dots (4.45)$$

and R is the rainrate in millimeter per hour.

The parameter depends on the rain intensity and expressed in units of per millimeter.

4.5. ATTENUATION DUE TO DIFFERENT SHAPES

The propagation constants associated with the horizontal and vertical scattering amplitudes given by ref /9/ as

$$K_{V,H} = K_0 + \frac{2\pi}{k_0} \int_0^{\infty} F_{V,H}(\underline{i}, \underline{i}) \bar{a} \, d\bar{a} \quad \dots (4.46)$$

Where $\bar{a} \cdot d\bar{a}$ is the number of drops per cubic metre with radii between a and $a+da$, and k_0 is the free space propagation constant.

Since raindrops behave as Rayleigh scatterers for frequencies up to at least 30GHZ, Howarth, Watson and McEwan /19/ have developed a simple replacement

for equ.(4.46) base on Rayleigh theory. In it, they assume that the shape of the raindrops is not important and that the raindrops may be described by a quantity $A_{V,H}$. This assumption has been verified for spheroids with nearly spherical shapes.

In the Haworth, Watson and McEwan formulation,

$$K_{V,H} = \frac{2\pi}{\lambda} + \frac{3\pi V}{\lambda} A_{V,H} \quad \dots(4.47)$$

Where λ is the free-space wavelength in meters and V is the total volume of ice (in cubic metres) in 1 m^3 of cloud. The quantities A_V and A_H have unites of m^{-3} , and depend on the crystal geometry and the refractive index of ice.

When K_V and K_H are known, the attenuation may be calculated for arbitrarily polarized waves propagating through raindrops.

Attenuation is given by

$$A_{V,H} = 8.686 \text{ Im} (K_{V,H}) \times 10^5 \text{ dB/km} \quad \dots(4.48)$$

In order to obtain $A_{V,H}$ for different shapes, we are changing values of L 's by using ref /6/.

CHAPTER V

APPLICATIONS

5.1. THE COMPUTER PROGRAM

The program to compute the attenuation due to different shapes such as circular disks, thin cylinder, sphere and so on, is written in FORTRAN 77.

The program is written as a master program and the following subroutines :

SUBROUTINE BESCl(X,Y)- The subroutine which calculates the volume integral of circular disk. BESCl(X) calculates $j_1(X(I))/X(I)$ where j_1 is the Bessel function of 1st order. The algorithm is from Abramowitz and Stegun 9.4.1 and 9.4.6. The accuracy is $1.0E-08$.

SUBROUTINE GRAPHIC- The subroutine which plots the results.

SUBROUTINE SIGMA- The subroutine which computes the normalized cross-sections of circular disk, thin cylinder and sphere.

The suggested algorithm for the solution is drawn as a flow chart in Fig.5.1.

The sequence of solution procedure was arranged in such a way that the solution will take the minimum computation time, the minimum storage size.

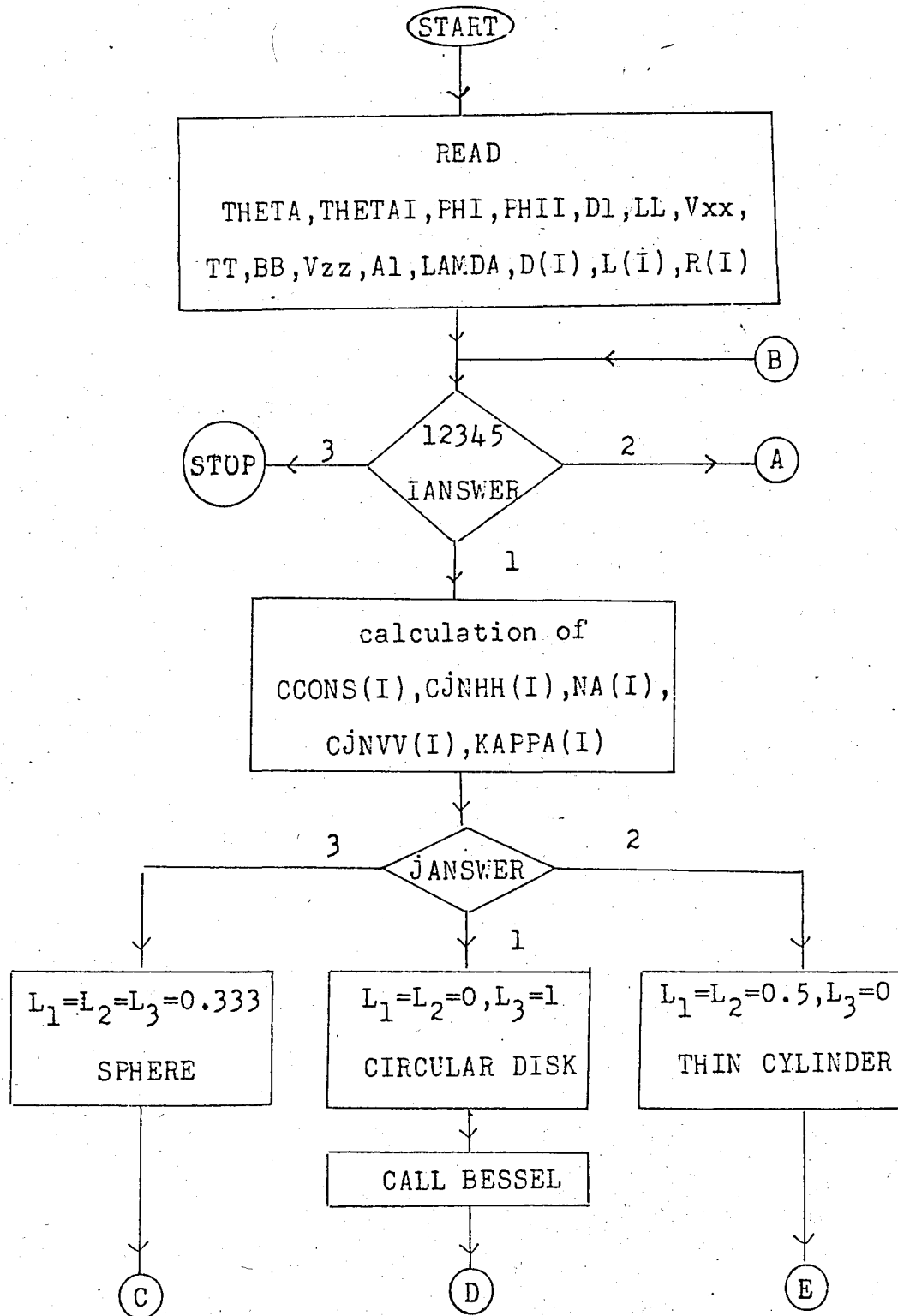


Fig.5.1. Flow chart for the program

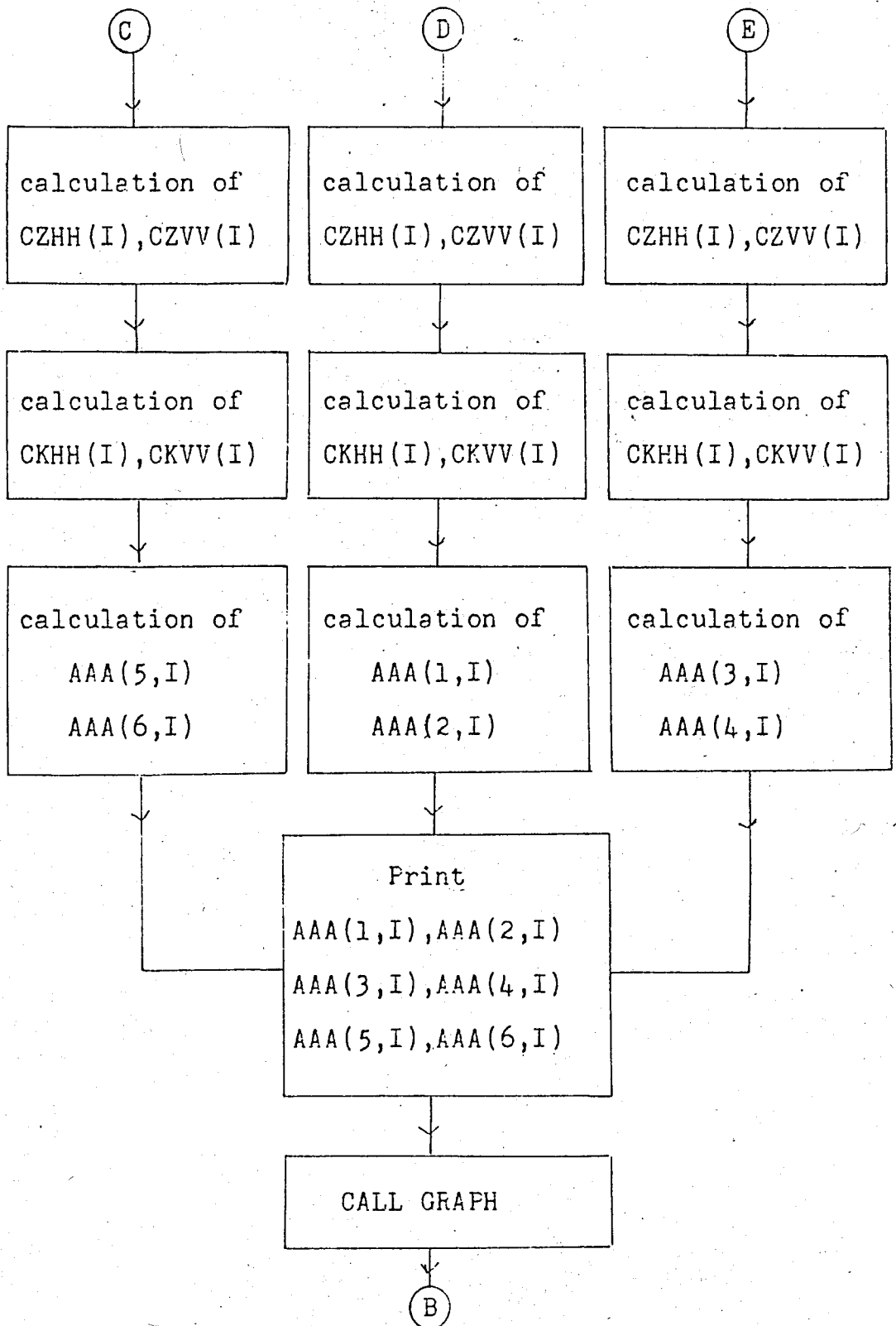
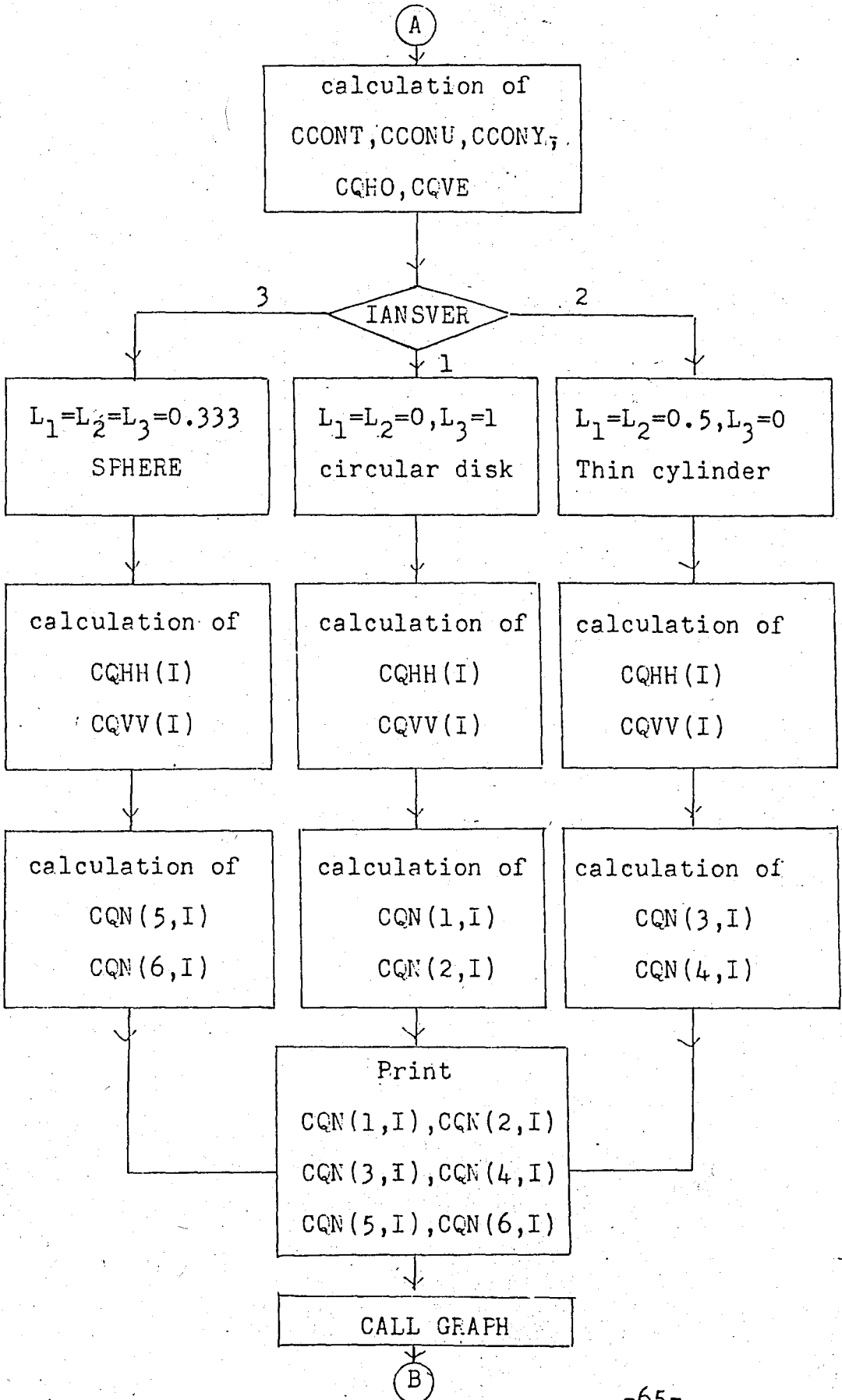


Fig.5.1. The flow chart (continued)

Fig.5.1. The flow chart(continued)



PROGRAM THIS IS (INPUT, OUTPUT, TAPE5=INPUT, TAPE6=OUTPUT)

```
*****
*
* CALCULATION OF HORIZONTAL AND VERTICAL ATTENUATION DUE
* TO ARBITRARILY ORIENTED DIFFERENT SHAPES;
*
* (A) CIRCULAR DISC
* (B) THIN CYLINDER
* (C) SPHERE
*
* X AND Y ARE IN LOGARITMIC SCALE
*
```

```
*****
IMPLICIT COMPLEX (C)
INTEGER IANSWER
REAL KAPPA(30), R(30), NA(30), RR(6,30), L1, L2, L3, LAMDA, LL
COMMON/AAA/T, TI, PHI, PHII, LL, VXX, TT, BB, VZZ, LAMDA
DIMENSION CKHH(30), CKVV(30), AAA(5,30), IN(6)
READ(5,*) T, TI, PHI, PHII, TT, LL, D1, B, VXA, VZZ, LAMDA, A1
DO 12345 IANSWER=1,3
IF (IANSWER.EQ.1) THEN
GO TO 45
ELSE IF (IANSWER.EQ.2) THEN
CALL SIGMA
GO TO 12345
ELSE IF (IANSWER.EQ.3) THEN
GO TO 555
ENDIF
```

45 PI=3.14159265

```
***** DATA R SHOWS RAINFALL RATE *****
DATA R/5., 10., 15., 20., 25., 30., 35., 40., 45., 50., 55., 60., 65., 70.
75., 80., 85., 90., 95., 100., 105., 110., 115., 120., 125., 130., 135.
140., 145., 150./
```

```
*** PKO=PROPAGATION CONSTANT, LAMDA=WAVELENGTH *****
PKO=(2*PI)/LAMDA
```

```
*** CM=REFRACTIVE INDEX OF THE PRECIPITATION *****
CM=(5.531+2.342)
```

```
T=T*PI/180
TI=TI*PI/180
PHI=PHI*PI/180
CK1=1./(1.+L1*(CM**2-1.))
CK2=1./(1.+L2*(CM**2-1.))
CK3=1./(1.+L3*(CM**2-1.))
CCONS=PKO*PKO*(CM*CM-1.)/(4.*PI)
CKHH=CCONS*(SIN(T)*SIN(T)*SIN(PHI)*SIN(PHI)*CK1+
COS(T)*COS(T)*SIN(PHI)*SIN(PHI)*CK2+COS(PHI)*COS(PHI)*
CK3)
CKVV=CCONS*(CK1*((SIN(TI)*COS(T)-COS(TI)*
SIN(T)*COS(PHI))**2)+CK2*((COS(TI)*COS(T)*COS(PHI)+
SIN(TI)*SIN(T))**2)+CK3*((COS(TI)*SIN(PHI))**2))
```

```
DO 50 I=1,30
KAPPA(I)=S2.*R(I)**(-.21)
NA(I)=.16*EXP(-KAPPA(I)*A1)
```

```

PRINT*,KAPPA(I)
50 CONTINUE
DO 23456 JANSWER=1,3
IF (JANSWER.EQ.1) THEN
L1=1
L2=0
L3=0
U=PK0+D1/2*VXX
CALL RESC1(U,P)
PRINT*,U,P
VP1=(.5*PI*D1*D1*TT)*P/U
CZHH=CJNHH*VP1
CZVV=CJNVV*VP1
DO 100 I=1,30
CKHH(I)=PK0+(2*PI/PK0)*(CZHH*NA(I))
CKVV(I)=PK0+(2*PI/PK0)*(CZVV*NA(I))
100 CONTINUE
DO 200 I=1,30
AAA(1,I)=8.635*AIMAG(CKHH(I))*1.0E+5
AAA(2,I)=8.635*AIMAG(CKVV(I))*1.0E+5
*** * AA(1,I) SHOWS HORIZONTAL ATTENUATION DUE TO CIRCULAR D
*** * AA(2,I) SHOWS VERTICAL ATTENUATION DUE TO SAME SHAPE
PRINT*, 'R(I)',R(I)
PRINT*, 'AAA(1,I)',AAA(1,I)
PRINT*, 'AAA(2,I)',AAA(2,I)
200 CONTINUE
ELSE IF (JANSWER.EQ.2) THEN
L1=0
L2=.5
L3=.5
VP2=(.5*D1*DB*SIN(PI*PK0*LL*VZZ*.5))/(PK0*VZZ*.5)
CZHH=CJNHH*VP2
CZVV=CJNVV*VP2
DO 120 I=1,30
CKHH(I)=PK0+(2*PI/PK0)*(CZHH*NA(I))
CKVV(I)=PK0+(2*PI/PK0)*(CZVV*NA(I))
120 CONTINUE
DO 270 I=1,30
AAA(3,I)=5.685*AIMAG(CKHH(I))*1.0E+5
AAA(4,I)=5.635*AIMAG(CKVV(I))*1.0E+5
PRINT*, 'R(I)',R(I)
PRINT*, 'AAA(3,I)',AAA(3,I)
PRINT*, 'AAA(4,I)',AAA(4,I)
*****
AAA(3,I) SHOWS HORIZONTAL ATTENUATION DUE TO THIN CYLINDER
AAA(4,I) SHOWS VERTICAL ATTENUATION DUE TO THIN CYLINDER
*****
270 CONTINUE
ELSE
L1=.375
L2=L3=L1
VP3=((4/3)*PI*(D1*D1*D1))/3
CZHH=CJNHH*VP3
CZVV=CJNVV*VP3
DO 170 I=1,30
CKHH(I)=PK0+(2*PI/PK0)*(CZHH*NA(I))
CKVV(I)=PK0+(2*PI/PK0)*(CZVV*NA(I))

```

```

07 CONTINUE
   DO 230 I=1,30
   AAA(5,I)=3.635*AIMAG(CKHH(I))*1.0E+10
   AAA(6,I)=3.635*AIMAG(CKVV(I))*1.0E+10
   PRINT*,'R(I)',R(I)
   PRINT*,'AAA(5,I)',AAA(5,I)
   PRINT*,'AAA(6,I)',AAA(6,I)
*****
AAA(5,I) SHOWS HORIZONTAL ATTENUATION DUE TO SPHERE
AAA(6,I) SHOWS VERTICAL ATTENUATION DUE TO SAME SHAPE
*****
07 CONTINUE
   ENDIF
08 CONTINUE
   DO 400 I=1,50
   RR(1,I)=RR(2,I)=RR(3,I)=RR(4,I)=RR(5,I)=RR(6,I)=R(I)
   IN(1)=IN(2)=IN(3)=IN(5)=IN(6)=50
   CALL GRAPH (110,50,RR,AAA,IN,1,c)
   FORMAT(1H1)
   FORMAT(G12.4,2X,G12.4)
05 CONTINUE
05 STOP
   END

```

* SUBROUTINE BESSEL CALCULATES THE VOLUME INTEGRAL OF
* CIRCULAR DISC
*

SUBROUTINE BESC1(X,Y)

BESC1(X) CALCULATES $J_1(X)/X$ WHERE J_1 IN THE BESSEL
FUNCTION OF 1ST ORDER. THE ALGORITHM IS FROM ABRAMOWITZ AND
STEGUN 9.4.1 & 9.4.6. THE ACCURACY IS $1.0E-02$.

DIMENSION A(7),B(7),C(7)

PRINT*, '-----X=', X

IF(X.GT.3.0) GO TO 40

IF(X.LT.1.0E-05) GO TO 30

A(1)=.5

A(2)=-.5624998E0

A(3)=+.2109357E0

A(4)=-.3954269E-01

A(5)=+.443319E-02

A(6)=-.31761E-03

A(7)=+.1109E-04

Z=(X/3.0)**2

Y=A(1)

Z1=Z

DO 20 I=1,3

Y=A(I+1)*Z1+Y

Z1=Z1*Z

CONTINUE

RETURN

30 Y=.5

PRINT*, '*****Y*****', Y

RETURN

40 B(1)=-.7973645E0

B(2)=-.156E-05

B(3)=-.1659667E-01

B(4)=-.171055E-02

B(5)=-.249511E-02

B(6)=-.113653E-02

B(7)=-.20033E-03

C(2)=+.1249961E0

C(3)=-.5650E-04

C(4)=-.537379E-02

C(5)=-.74348E-03

C(6)=+.72324E-03

C(7)=-.29168E-03

F1=B(1)

```

C  SUBROUTINE GRAPHIC
C  IX : DIMENSION OF X
C  IY : DIMENSION OF Y
C  X  : INDEPENDANT VARIABLE
C  Y  : DEPENDANT VARIABLE
C  IN : NUMBER OF POINT
C  NL : LOG INDICATOR (NL=0 X AND Y NORMAL, NL=1 X AND Y LOG,
C  NL=2 ONLY X LOG, NL=3 ONLY Y LOGARITHMIC.
C  IDIM: NUMBER OF GRAFIC
C

```

```

SUBROUTINE GRAPH (IX,IY,X,Y,IN,NL,IDIM)
DIMENSION X(6,500),Y(6,500),U(11,1),V(56),D(12),E(12),IN(6)
CHARACTER*1 A(56,111),F(111)
REAL MIN,MAX,MIN1,MAX1,INCX,INCY
DO 5 I=1,56
DO 5 J=1,111
X(I,J)=' '
5 CONTINUE
IF (IX.GT.111.OR.IX.LT.2) IX=111
IF (IY.GT.56.OR.IY.LT.2) IY=56
IF (NL.EQ.1.OR.NL.EQ.2) THEN
DO 10 N=1,IDIM
DO 10 I=1,IN(N)
IF (X(N,I).NE.0) THEN
X(N,I)=ABS(X(N,I))
X(N,I)=ALOG10(X(N,I))
ENDIF
10 CONTINUE
ENDIF
IF (NL.EQ.1.OR.NL.EQ.3) THEN
DO 15 N=1,IDIM
DO 15 I=1,IN(N)
IF (Y(N,I).NE.0) THEN
Y(N,I)=ABS(Y(N,I))
Y(N,I)=ALOG10(Y(N,I))
ENDIF
15 CONTINUE
ENDIF
DO 20 I=1,IX
F(I)='- '
20 CONTINUE
DO 25 I=1,IX,10
F(I)='+'
25 CONTINUE
MIN=X(1,1)
MAX=X(1,1)
MIN1=Y(1,1)
MAX1=Y(1,1)
DO 30 N=1,IDIM
DO 30 I=1,IN(N)
IF (X(N,I).GT.MAX) MAX=X(N,I)
IF (X(N,I).LT.MIN) MIN=X(N,I)
IF (Y(N,I).GT.MAX1) MAX1=Y(N,I)
IF (Y(N,I).LT.MIN1) MIN1=Y(N,I)
30 CONTINUE

```

```

INCX=(MAX-MIN)/(IX-1)
INCY=(MAX1-MIN1)/(IY-1)
J(1)=MIN
V(1)=MIN1
DO 40 I=1,IX-1
U(I+1)=U(I)+INCX
40 CONTINUE
DO 45 I=1,IY-1
V(I+1)=V(I)+INCY
45 CONTINUE
DO 55 M=1,IDI
DO 60 I=1,IN(X)
M=1
DIFF=ABS(X(M,1)-U(1))
DO 50 J=1,IX-1
IF (ABS(X(M,I)-U(J+1)).LT.DIFF) THEN
DIFF=ABS(X(M,I)-U(J+1))
M=J+1
ENDIF
50 CONTINUE
L=1
DIFF1=ABS(Y(M,I)-V(1))
DO 53 J=1,IY-1
IF (ABS(Y(M,I)-V(J+1)).LT.DIFF1) THEN
DIFF1=ABS(Y(M,I)-V(J+1))
L=J+1
ENDIF
55 CONTINUE
IF (Y.EQ.1) A(L,M,1)='+'
IF (Y.EQ.2) A(L,M,1)='S'
IF (Y.EQ.3) A(L,M,1)='Q'
IF (Y.EQ.4) A(L,M,1)='G'
IF (Y.EQ.5) A(L,M,1)='*'
IF (Y.EQ.6) A(L,M,1)='B'
60 CONTINUE
65 CONTINUE
L2=0
L3=0
DO 70 I=1,IY/5
L2=L2+1
IF (VL.EQ.1.OR.VL.EQ.3) D(L2)=10**V(I)
IF (VL.NE.1.AND.VL.NE.3) D(L2)=V(I)
70 CONTINUE
DO 75 I=1,IX/10
L3=L3+1
IF (VL.EQ.1.OR.VL.EQ.2) E(L3)=10**U(I)
IF (VL.NE.1.AND.VL.NE.2) E(L3)=U(I)
75 CONTINUE
IF (VL.EQ.1.OR.VL.EQ.2) THEN
DO 80 M=1,IDI
DO 85 I=1,IN(X)
X(M,I)=10**X(M,I)
80 CONTINUE
ENDIF
IF (VL.EQ.1.OR.VL.EQ.3) THEN
DO 85 M=1,IDI

```

```

00 35 I=1,IN(M)
Y(M,I)=10*Y(M,I)
85 CONTINUE
ENDIF
K7=((IY-1)/5)*5+1
IP=(IY-1)/10+1
PRINT 95
00 90 I=IY,1,-1
IF (I.EQ.K7) THEN
K7=K7-5
L=I/5+1
PRINT 100,D(L),(A(I,J),J=1,IX)
GO TO 90
ENDIF
PRINT 105,(A(I,J),J=1,IX)
90 CONTINUE
PRINT 110,(F(I),I=1,IX)
PRINT 115,(G(I),I=1,IP)
RETURN
95 FORMAT(1H1,/)
100 FORMAT(3X,1PE10.2,1X,'+',111A1)
105 FORMAT(14X,' I ',111A1)
110 FORMAT(15X,111A1,/)
115 FORMAT(11X,11(1PE9.2,1X),1PE9.2,/)
END

```

```

C *****
C *
C * SUBROUTINE SIGMA IS A PLOT PROGRAM FOR NORMALISED HORI
C * TAL AND VERTICAL CROSS-SECTIONS OF;
C *
C * (A) CIRCULAR DISC
C * (J) THIN CYLINDER(ROJ)
C * (C) SPHERE
C *
C * X AND Y ARE IN NORMAL SCALE
C *
C *****

```

```

SUBROUTINE SIGMA
IMPLICIT COMPLEX (C)
COMMON/AAA/T, TI, PHI, PHII, LL, VXX, IT, BB, VZZ, LAMDA
INTEGER ANSWER
REAL LAMDA, L1, L2, L3, D(10), LL, BB, IT, DV(5, 10)
DIMENSION CWHH(10), CVVV(10), CWHH(10), CVVV(10), IN(5), CWH
+ ,VDL(10)
DATA D/1., 2., 3., 4., 5., 6., 7., 8., 9., 10./
PI=3.14159265
PKO=(2*PI)/LAMDA
CH=(5.317, -2.869)
T=T*PI/180
TI=TI+PI/180
PHI=PHI*PI/180
PHII=PHII*PI/180
CK1=1./(1.+L1*(CH**2-1.))
CK2=1./(1.+L2*(CH**2-1.))
CK3=1./(1.+L3*(CH**2-1.))
CCONS=PKO*PKO*PKO*PKO*(CH**2-1.)/(4.*PI)
CCONT=(-COS(TI)*COS(PHI)*SIN(PHII)-COS(PHII)*SIN(PHI)*
COS(T))*CK1+(SIN(PHI)*SIN(PHII)+COS(PHI)*COS(PHII))*CK2
+ (SIN(T)*SIN(PHI)*COS(PHII)-SIN(T)*SIN(PHII)*COS(PHI))
*CK3
CCOQU=ABS(CCONT)
CQHQ=CCONS*(CCOQU)**2
CQNV=(-COS(T)*COS(TI)*COS(PHI)*COS(PHII)-COS(T)*COS(TI)
SIN(PHI)*SIN(PHII)-SIN(T)*SIN(TI))*CK1+(COS(TI)*SIN(PHI)
COS(PHII)-COS(TI)*SIN(PHII)*COS(PHI))*CK2+(-COS(TI)*SIN(
COS(PHI)*COS(PHII)-SIN(T)*COS(TI)*SIN(PHI)*SIN(PHII)+COS
SIN(TI))*CK3
CQNY=ABS(CQNV)
CQVE=CCONS*(CQNY)**2
D=34567 ANSWER=1/3
IF (ANSWER.EQ.1) THEN
L1=1
L2=L3=0
DO 100 I=1, 10
VDL(I)=(PI)**2*(D(I)**2)**2*TT**2/36
CWHH(I)=CQHQ*VDL(I)
CVVV(I)=CQVE*VDL(I)

```

```

C   CQN(1,I) INDICATES HORIZONTALY NORMALISED CROSS-SECTION OF SP
C   CQN(2,I) INDICATES VERTICALLY NORMALISED CROSS-SECTION OF SPHE
C   *****
C   PRINT*, 'CQN(1, I)', CQN(1, I)
C   PRINT*, 'CQN(2, I)', CQN(2, I)
100 CONTINUE
C   ELSE IF (ANSWER.EQ.2) THEN
C   L1=0
C   L2=L3=.5
C   DO 200 I=1,10
C   VOL(I)=(PI**2*D(I)**2*SB**2*LL**2)/4.
C   CQH(I)=CQHC*VOL(I)
C   CQN(3, I)=CQH(I)/(PI*D(I)*SB/2)
C   CQV(I)=CQVC*VOL(I)
C   CQN(4, I)=CQV(I)/(D(I)*LL)
C   *****
C   CQN(3,I) SHOWS THE HORIZONTAL NORMALISED CROSS-SECTION OF ROD
C   CQN(4,I) SHOWS THE VERTICAL NORMALISED CROSS-SECTION OF ROD
C   *****
C   PRINT*, 'CQN(3, I)', CQN(3, I)
C   PRINT*, 'CQN(4, I)', CQN(4, I)
200 CONTINUE
C   ELSE
C   L1=L2=L3=.333
C   DO 300 I=1,10
C   VOL(I)=(PI**2*((D(I)**2)**2)*TT**2)
C   CQH(I)=CQHC*VOL(I)
C   CQN(5, I)=(CQH(I)/(PI*D(I)**2/4))*1.0E+3
C   CQV(I)=CQVC*VOL(I)
C   CQN(6, I)=CQV(I)/(PI*D(I)**2/4)
C   PRINT*, 'CQN(5, I)', CQN(5, I)
C   PRINT*, 'CQN(6, I)', CQN(6, I)
C   *****
C   CQN(5,I) SHOWS THE HORIZONTAL NORMALISED CROSS-SECTION OF SPH
C   CQN(6,I) SHOWS THE VERTICAL NORMALISED CROSS-SECTION OF SPHE
C   *****
300 CONTINUE
C   ENDDIF
34567 CONTINUE
C   DO 400 I=1,10
400 DD(1,I)=DD(2,I)=DD(3,I)=DD(4,I)=DD(5,I)=DD(6,I)=D(I)
C   IN(1)=IN(2)=IN(3)=IN(4)=IN(5)=IN(6)=10
C   CALL GRAPH (110,50,00,CQN,IN,6,6)
C   STOP
3   FORMAT(1H1)
9   FORMAT(3I2,4,2X,3I2,4)
C   END

```

5.2. (NUMERICAL RESULTS AND DISCUSSION

We are dealing with normalized cross-sections versus raindrop diameter. In the other part of the main program, we are investigating how attenuation varies with respect to rainfall rate.

Figures (5.1), (5.2) and (5.3) give us information about normalized cross-sections of circular disk, thin cylinder and sphere. In Fig.5.1, $\#$ character indicates both horizontal and vertical normalized cross-sections of sphere. Same is true for sphere in Fig.5.2. While diameter of sphere is increasing, the vertical and horizontal normalized cross-sections of sphere are constant and equal to each other. Whereas the other characters \star, ζ for circular disk or $\checkmark, \&$ for thin cylinder, show vertical and horizontal normalized cross-sections of those particles. In Fig.5.3, y axis is in logarithmic scale. By using ref/6/, it is also possible to investigate the variation of normalized cross-sections of any shapes.

Fig(5.4) gives us a comparison between thin cylinder and sphere. There are three different characters in that figure, (+) and (s) characters indicate attenuations due to thin cylinder vertically and horizontally respectively, whereas (&) character shows attenuation of sphere. It is clear that vertical and horizontal attenuations are equal to each other for sphere case.

In fig(5.5), sphere is comparing with circular disk. Again vertical and horizontal attenuations are showing with two characters for circular disk one is for sphere.

Figs (5,4) and (5.5) are good agreement with ref /3/ and /9/, From 10mm/hr up to 150mm/hr, attenuation is very high for millimetric wave propagation. The values of horizontal and vertical attenuations approach the results given by ref /9/. Fig.(5.6) indicates that attenuation is very high at low values of wavelength. This result is in a good agreement with ref/3/.

$\lambda = 5 \text{ mm.}$

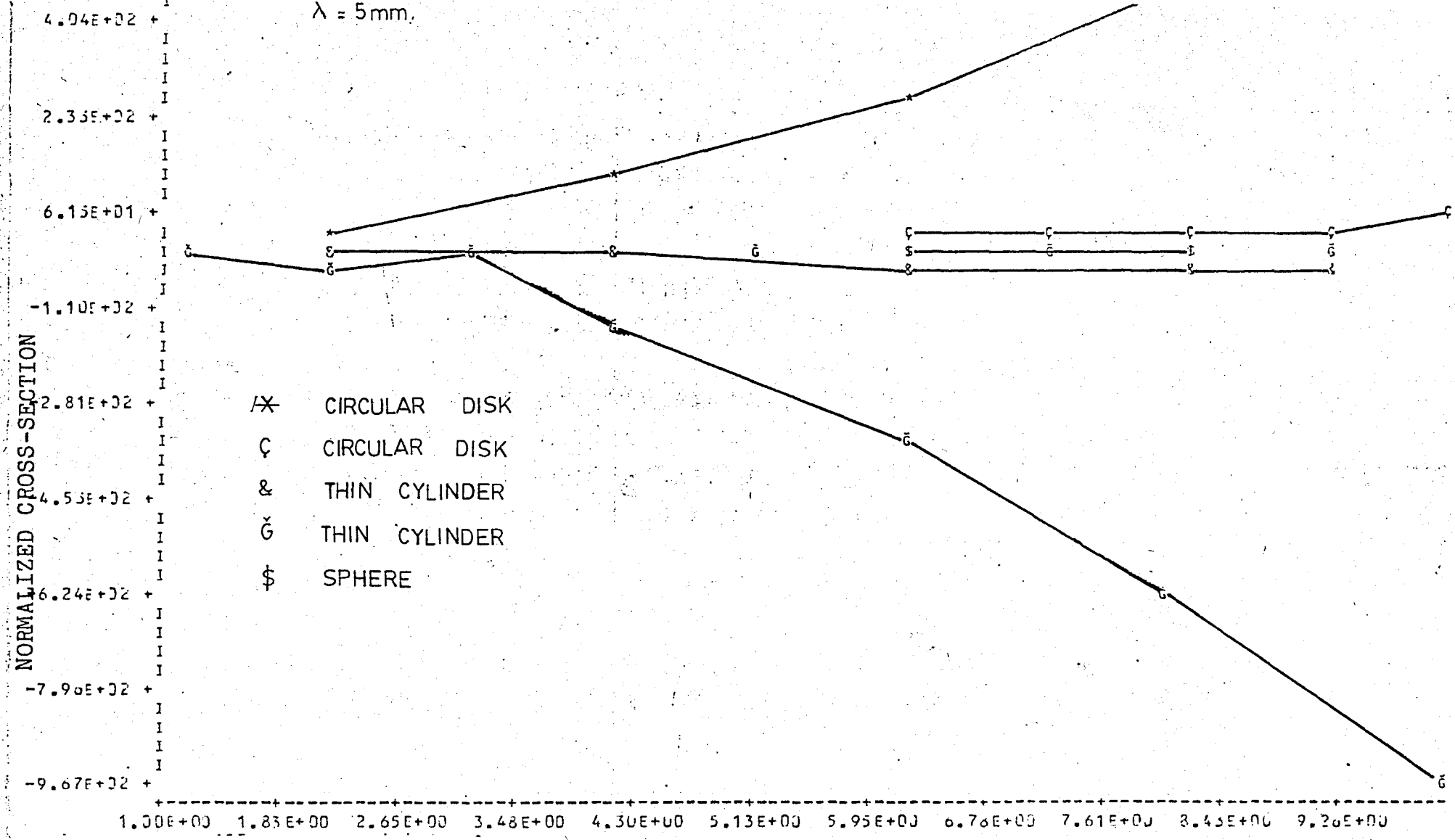


Fig 51 Normalized cross-section vs raindrop diameter.

Diameter

$\lambda = 9 \text{ mm}$

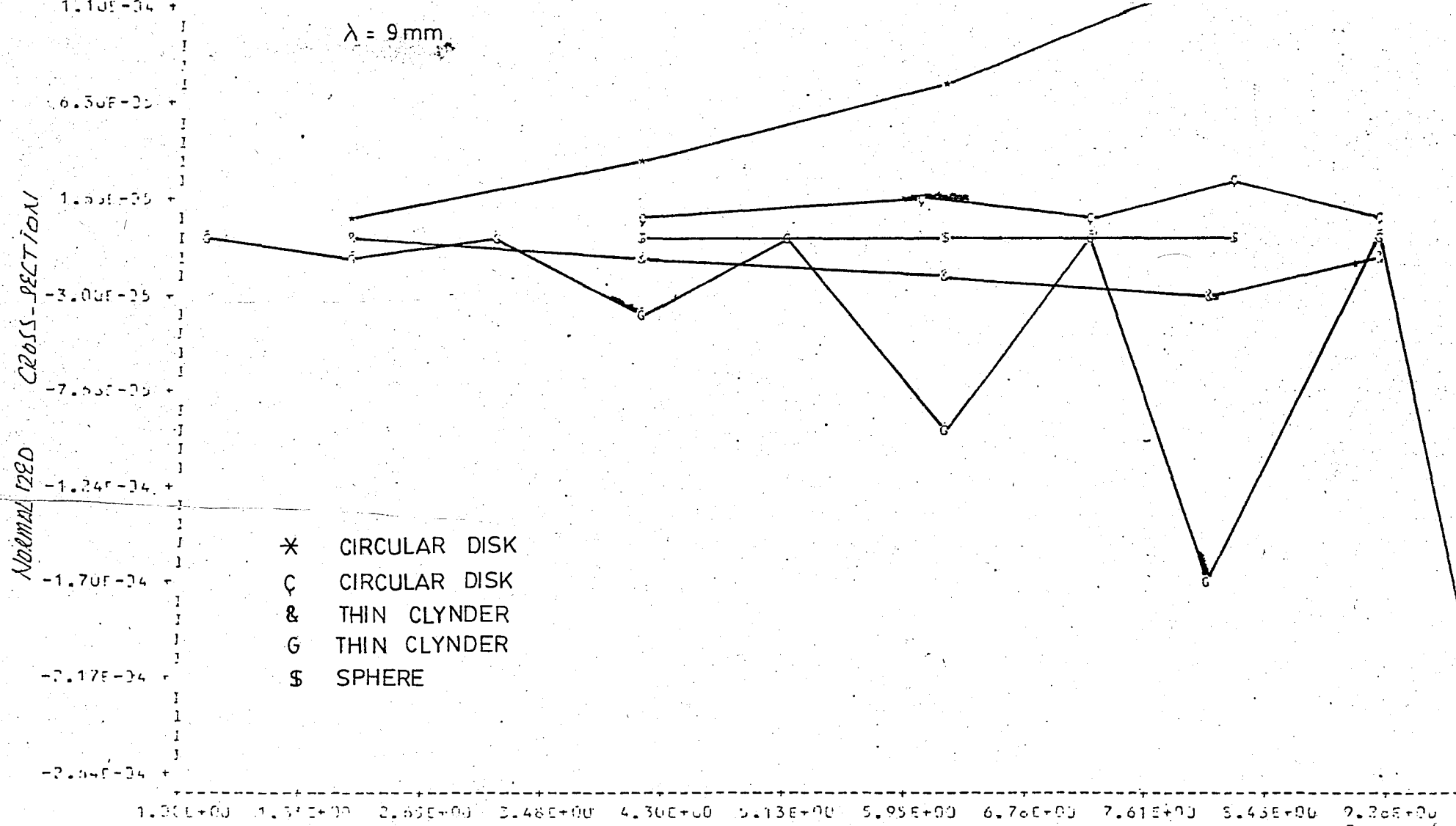


Fig. 5.2 Normalized cross-section vs Raindrop diameter Diameter

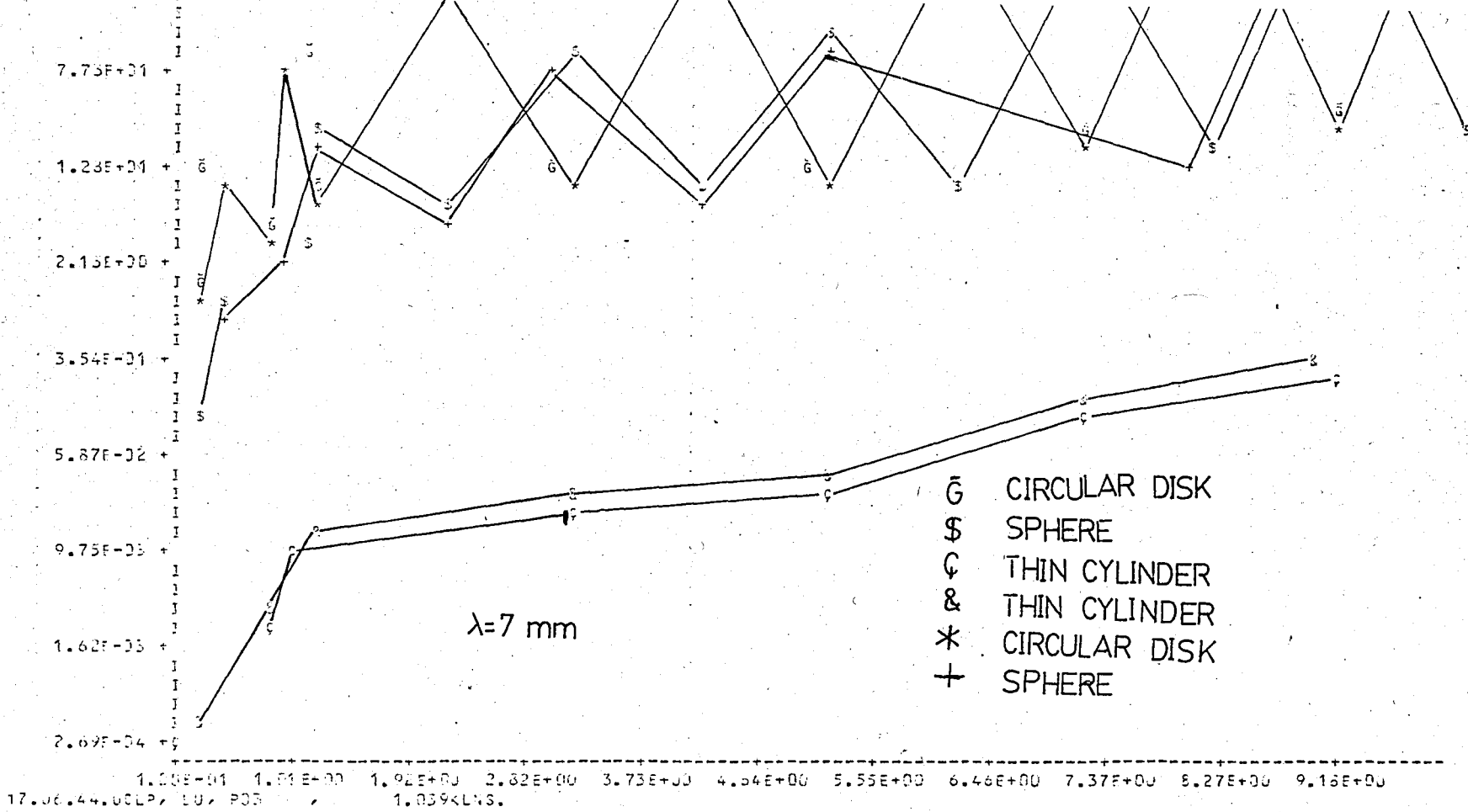


Fig 5.3 Normalized cross section vs Raindrop diameter

& SPHERE
 + THIN CYLINDER (Ver. Pol.)
 $\lambda = 8 \text{ mm.}$

ATTENUATION (dB/km)

1.16E+03
 5.15E+02
 2.29E+02
 1.02E+02
 4.54E+01
 2.02E+01
 8.98E+00
 3.99E+00
 1.78E+00

5.00E+00 6.33E+00 7.35E+00 1.25E+01 1.74E+01 2.33E+01 3.25E+01 4.40E+01 6.07E+01 8.00E+01 1.10E+02

Fig 5.4 Attenuation YS Rainfall rate mm/hr

☉ SPHERE

$\lambda = 9\text{mm}$

ATTENUATION (dB/km)

6.75E+00
2.02E+00
6.42E-01
1.97E-01
6.07E-02
1.87E-02
5.73E-03
1.77E-03
5.44E-04

5.10E+00 6.83E+00 9.33E+00 1.28E+01 1.74E+01 2.38E+01 3.29E+01 4.44E+01 6.07E+01 8.29E+01 1.13E+02

Fig 5 5 Attenuation VS Rainfall rate

Rainfall rate mm/hr

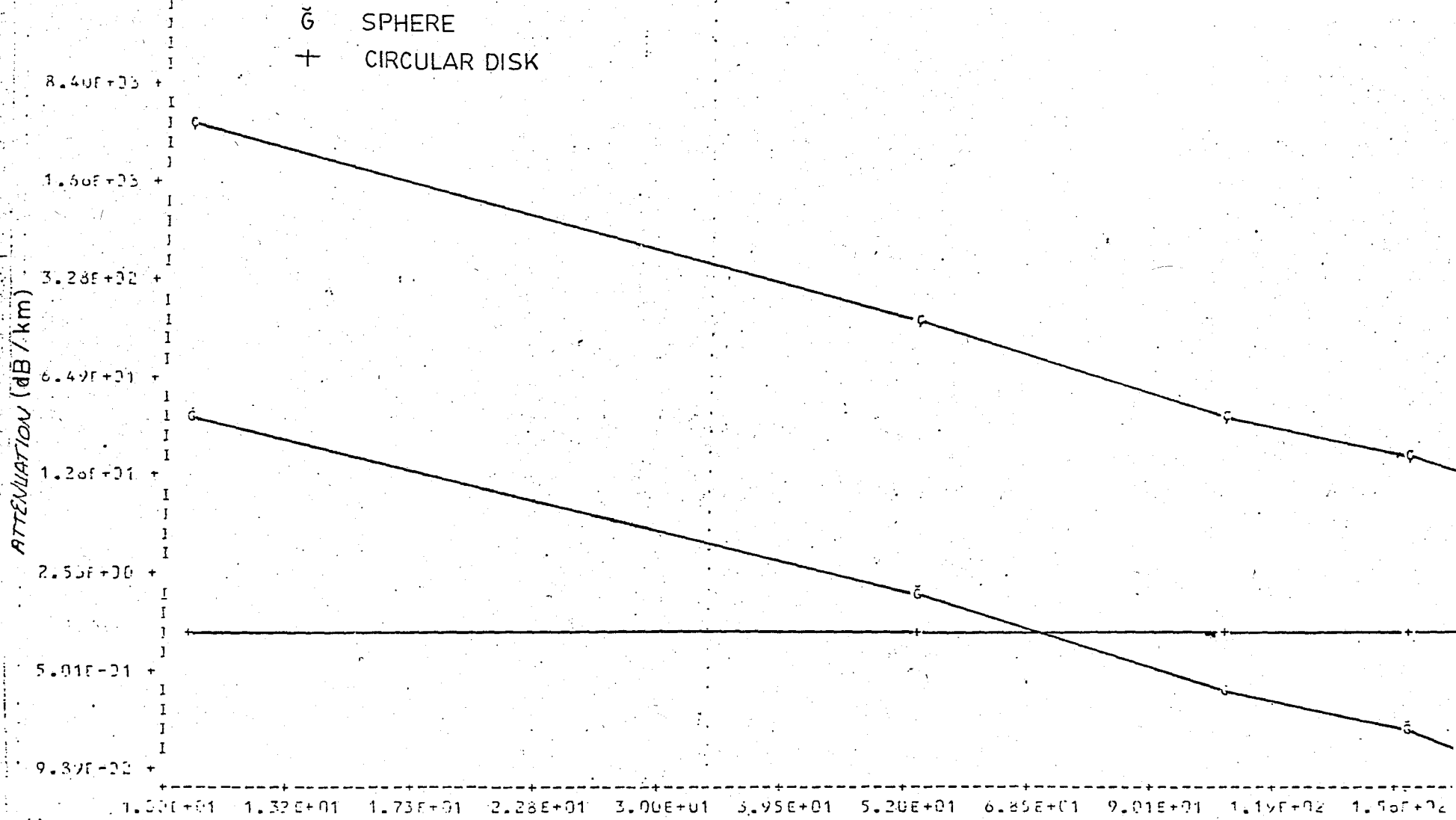


Fig 5.6 Attenuation vs wavelength

Wavelength λ

CONCLUSIONS

Rain imposes a limitation on millimeter wavelengths, since attenuation by rain is high. In the space-to-space, space-to-ground, or ground-to-space communication at the millimetric wavelength, the effects of fog, cloud and other aerosols can be detected with a carefully designed experiment. In other words, in other applications, such as fog and clouds studies, the attenuation is tolerable.

This work shows the attenuation in rain due to different shapes such as circular disk, thin cylinder, sphere at the millimetric wave propagation.

REFERENCES

- /1/ E.E.Altshuler, J.V.Falcone, Jr.,K.N.Wulfsberg,
"Atmospheric effects on propagation at milli-
meter wavelengths"; IEEE Spectrum, July 1968.
- /2/ R.G.Medhurst,"Rainfall attenuation of centime-
ter waves: Comparison of theory and measurement",
IEEE Transaction on Antennas and Propagation,
vol. AP-13, no.4, pp.550-563, July 1965.
- /3/ R.L.Mitchell, "Radar Meteorology at millimeter
wavelengths", Electronics Research Laboratory,
Aerospace Report no. TR-669 (6230-46)-9, June
1966
- /4/ A.Ishimaru, Wave propagation and scattering in
Random Media, Academic Press, New York, 1978.
- /5/ M.Kerker, The scattering of light and other
electromagnetic Radiation, Academic, New York
1969.

- /6/ H.C.Van de Hulst, Light scattering by small particles, Dover, New York, 1957.
- /7/ Ş.S.Şeker, "Radar cross-section of thin dielectric bodies", IEEE Proceedings.H.Vol.133, No.4 August 1986
- /8/ D.Atlas, "Advances in Radar meteorology", Advan. Geophys., vol. 10, pp. 317-478, 1964.
- /9/ N.K.Uzunoğlu, B.G.Evans, A.R.Holt, "Sattering of electromagnetic radiation by precipitation particles and propagation characteristics of terrestrial and space communication systems", IEEE Proceeding, Vol.124, No.5, May 1977.
- /10/ C.W.Bostian, J.E.Allnutt, "Icecrystal depolarisation on satellite-earth microwawe radio paths", IEEE, Proc., Vol.26, No.10, October 1979.
- /11/ D.M.Le VINE, "The radar cross-section of dielectric disks", IEEE Trans. on Antennas and Propagation, Vol.AP-32, No.1, January 1984.

- /12/ R.Schiffer and K.O.Thielheim,"Light scattering by dielectric needles and disks", J.Appl.Phys. 50(4), April 1979.
- /13/ A.R.Holt, N.K.Uzunoğlu, and B.G.Evans,"An integral equation solution to the scattering of spheroids and ellipsoids", IEEE Trans. on Antennas and Propagation, Vol.AP-26,No.5, September 1978.
- /14/ D.V.Rogers and R.L.Olsen,"Tables of scattering functions for propagation in rain at frequencies between 1 and 1000 GHZ", Communications Res.Center, Dep. of communications, Ottawa, on, Canada, CRC Rep. in preparation.
- /15/ P.S.Ray,"Broadband complex-refractive indices of ice and water", Appl. Opt.,Vol.11, pp.1836-1844, Aug 1972.
- /16/ J.O.Laws and D.A.Farsons,"The relation of raindrop-size intensity",Trans. Amer. Geophys. Union, Vol.24, pp.452-465, 1943.

- /17/ D.T.Llewellyn-Jones, "Attenuation by rainfall in the submillimeter wave region", in Modern Topics in microwave propagation and Air-sea Interaction, A.Zancla. Ed.Dordrecht, Holland: Reidel, pp.285-291, 1973.
- /18/ J.Joss, J.C.Thams, and A.Waldvogel, "The variation of raindrop size distributions Locorno", in Proc.Int.Conf.Cloud.Physics, pp.369-373,1968.
- /19/ D.P.Haworth, P.A.Watson, and N.J.McEwan, "Model for the effect of electric fields on satellite-earth microwave radio propagation", Electronics Letters, vol.13, No.19, September 1977.
- /20/ K.Shimizu, "Modification of the Rayleigh-Debye approximation, "J.opt.Sci.Am., Vol.73, No.4, April 1983.

REFERENCES NOT CITED

- /1/ Proceeding of the IEEE, April 1966.
- /2/ D.C.Hogg and T.S.Chu, "The role of rain in satellite communications", Proc.IEEE, pp.1308-1330 Sept. 1963.
- /3/ K.N.Wulfsberg, "Sky noise measurements at millimeter wavelengths", Proc. IEEE. Vol 52, pp.321-322, Mar. 1964.
- /4/ R.Chad ha, J.A.Lane "Effect of scattering in measurements of rain attenuation by passive radiometry", Electron Lett. 13(7), 177, 178, 1977.
- /5/ A.M.Zavody, "Effect of scattering by rain on radio measurements at millimeter wavelengths", Proc. IEE, pp. 257-263, 1974.
- /6/ "Special issue on millimeter wave antenna and propagation", IEEE Trans. Antennas and Prop. Vol. AP-18.1970.

- /7/ R.K.Cane, "Propagation phenomena affecting satellite communication systems operating in the centimeter and millimeter wavelength Bands", Proc. IEEE, Vol.59, pp. 173-188, 1971.
- /8/ G.E.Weibel and H.O.Dressel, "Propagation studies in millimeter wave link systems", Proc. IEEE, Vol.55, pp. 497-513, 1967.
- /9/ D.B.Hodge, "Frequent scalling of Rainfall", IEEE Trans. on Antennas and propagation, Vol.AP-25, No.3, pp446, May 1977.
- /10/ D.P.Haworth, "Model for the effects of the electric field on satellite eart M.W. radio prop.", Electronic letter. pp. 342-343 No.13, 1977.
- /11/ P.A.Watson, and M.Arbabi; "Rainfall cross polarization at microwave frequencies", Proc. IEEE, 120, No.4, pp.413-418. April 1973.

- /12/ G.Brussaard, "A meteorological model for Rain-induced cross-polarization", IEEE Trans. on Antennas and propagation, Vol.AP-24, No.1, pp.5-11, January 1976.
- /13/ T.W.Harrold, "Attenuation of 8.6 mm wavelength Radiation in Rain", Proc.IEEE, Vol.114, pp.201-203, 1967.
- /14/ B.C.Blevis, R.M.Dohoo and K.S.McCormick, "measurement of Rainfall Attenuation at 8 and 15 GHz, IEEE Trans. Antennas and Prop., Vol. Ap-15, pp.394-403, 1967.
- /15/ J.A.Stratton, Electromagnetic Theory, McGraw-Hill, pp.554-573, New York 1941.
- /16/ D.Deirmendjian, "Scattering and polarization properties of water clouds and hazes in the visible and infrared" ;Appl. Opt., Vol.3, no.2, p.187, February 1964.

/17/ P.H.Wiley, W.L.Stutzman, and C.W.Bostian, "A new model for rain depolarisation", J.Rech.Atmos., pp. 147-153, 1974.

/18/ A.Tsolakis and W.L.Stutzman, "Calculation of ice depolarization on stellite radio paths", Radio Science, Vol.18, No.6, pp.1287-1293, November-December 1983.

/19/ J.E.Gordon, "Simple method for approximating Mie scattering", J.Opt. Soc. Am., Vol.2, No.2, February 1985.

APPENDIX

CALCULATION OF VOLUME INTEGRAL

The volume integral V_p is defined in the reference frame by

$$V_p = \int_{\text{Volume}} e^{jk_0 \underline{v} \cdot \underline{x}'} dx' \quad \dots (A1)$$

$$\text{with } \underline{v} = \underline{i}^0 - \underline{c}^0 = V_x \underline{x}^0 + V_y \underline{y}^0 + V_z \underline{z}^0 \quad \dots (A2)$$

$$\underline{x}' = x' \underline{x}^{01} + y' \underline{y}^{01} + z' \underline{z}^{01} \quad \dots (A3)$$

It is necessary to express variables \underline{x}' in the coordinates of reference frame but the integration is done in the primed system. Since \underline{x}^{01} , \underline{y}^{01} , \underline{z}^{01} are unit vectors in the primed system, they can be expressed in terms of the reference system using EULER ANGLE ROTATION. We use orthogonal transformation. For this transformation, we define a matrix which describes these rotations. The transformation matrix, $A(\phi, \theta, \chi)$, can be thought of as an operator which acting on the unpri-

med system. (see equ.4.6).

$$\begin{aligned}
 \underline{V} = (\underline{i} - \underline{q}) = & \hat{x}(-\sin\theta_i \cos\phi_i - \sin\theta_s \cos\phi_s) \\
 & + \hat{y}(-\sin\theta_i \sin\phi_i - \sin\theta_s \sin\phi_s) \\
 & + \hat{z}(-\cos\theta_i - \cos\phi_s) \quad \dots (A4)
 \end{aligned}$$

therefore

$$\begin{aligned}
 V_x = & -\sin\theta_i \cos\theta_i - \sin\theta_s \cos\phi_s \\
 V_y = & -\sin\theta_i \sin\phi_i - \sin\theta_s \sin\phi_s \\
 V_z = & -\cos\theta_i - \cos\theta_s \quad \dots (A5)
 \end{aligned}$$

In the primed coordinate system, integration is done. That is why we have to express \underline{V}' in terms of the reference coordinates (angles θ_i , ϕ_i and θ_s , ϕ_s and θ , ϕ , δ). Since V'_x , V'_y and V'_z are the projections of \underline{V}' on the x' , y' , and z' axes and since dot products are invariant under coordinate rotations, one can write

$$V'_x = \underline{V}' \cdot \hat{x}'$$

$$V'_y = \underline{V}' \cdot \underline{\hat{y}}'$$

$$V'_z = \underline{V}' \cdot \underline{\hat{z}}' \quad \dots (A6)$$

Where \hat{x}' , \hat{y}' and \hat{z}' are unit vectors along the x, y, and z axes of the scatterer as seen by an observer in the reference system.

$$\underline{\hat{x}}' = (\cos\delta \cos\phi - \sin\delta \sin\phi \cos\theta) \underline{\hat{x}}$$

$$+ (\cos\delta \sin\phi + \sin\delta \cos\phi \cos\theta) \underline{\hat{y}}$$

$$+ \sin\theta \sin\delta \underline{\hat{z}}$$

$$\underline{\hat{y}}' = -(\sin\delta \cos\phi + \cos\delta \sin\phi \cos\theta) \underline{\hat{x}}$$

$$+ (-\sin\delta \sin\phi + \cos\delta \cos\phi \cos\theta) \underline{\hat{y}}$$

$$+ \sin\theta \cos\delta \underline{\hat{z}}$$

$$\underline{\hat{z}}' = \sin\theta (\sin\phi \underline{\hat{x}} - \cos\phi \underline{\hat{y}}) + \cos\theta \underline{\hat{z}} \quad \dots (A7)$$

from which one can obtain

$$V'_x = (\alpha \sin \delta - \beta \cos \delta)$$

$$V'_y = (\beta \sin \delta + \alpha \cos \delta)$$

$$V'_z = \delta \quad \dots (A8)$$

Where $\alpha = \cos \theta [\sin \theta_i \sin(\phi - \phi_i) + \sin \theta_s \sin(\phi - \phi_s)]$

$$- \sin \theta [\cos \theta_i + \cos \theta_s]$$

$$\beta = \sin \theta_i \cos(\phi - \phi_i) + \sin \theta_s \cos(\phi - \phi_s)$$

$$\delta = - \sin \theta [\sin \theta_i \sin(\phi - \phi_i) + \sin \theta_s \sin(\phi - \phi_s)]$$

$$- \cos \theta \cos \theta_i + \cos \theta_s \quad \dots (A9)$$

Special cases

1) Scatterer has elliptical cross-section ($\gamma \neq 0$)

and thickness t . Volume integral, equ.(A1), is;

$$V_p = \frac{4\pi b}{k_o^2 V_x V_z} \sin\left(\frac{k_o t V_z}{2}\right) \left[\sum_{n=0}^{\infty} (-1)^n \frac{k_o b^2 V_y^2}{a V_x} j_{n+1}(k_o a V_x) \right]^n$$

$$\dots (A10)$$

Where $J_n(x)$ is the Bessel function of first kind of order n .

If thickness is so small, then Sinx/x , from equ. (A10), one can get

$$V_p = \frac{2\pi b t}{k_o v_x} \left[\sum_{n=0}^{\infty} (-1)^n \left(\frac{k_o b^2 v_y^2}{a v_x} \right) j_{n+1}(k_o a v_x) \right] \dots (A11)$$

And also, if we have a circular disk of radius $a=b$, then one can obtain for $n=0$

$$V_p = \frac{2\pi b t}{k_o v_x} j_1(k_o a v_x) \dots (A12)$$

In the Rayleigh limit, equ.(A12) becomes $V_p = a^2 t$ as expected.

2) If scatterer has elliptical cross-section and if it is sufficiently long and thin compared with the wavelength within (elliptical rod), then from equ.(A10), one can obtain

$$V_p = \pi a b l \text{Sinc}\left(\frac{k_o l v_z}{2}\right) \dots (A13)$$